

Anomalous scaling in fluid mechanics: The case of the passive scalar

Victor S. L'vov, Itamar Procaccia, and Adrienne L. Fairhall

Departments of Physics of Complex Systems and Chemical Physics, The Weizmann Institute of Science, Rehovot 76100, Israel
(Received 11 March 1994)

A mechanism for anomalous scaling in turbulent advection of passive scalars is identified as being similar to a recently discovered mechanism in Navier-Stokes dynamics [V. V. Lebedev and V. S. L'vov, JETP Lett. **59**, 577 (1994)]. This mechanism is demonstrated in the context of a passive scalar field that is driven by a rapidly varying velocity field. The mechanism is not perturbative, and its demonstration within renormalized perturbation theory calls for a resummation of infinite sets of diagrams. For the example studied here we make use of a small parameter, the ratio of the typical time scales of the passive scalar vs that of the velocity field, to classify the diagrams of renormalized perturbation theory such that the relevant ones can be resummed exactly. The main observation here, as in the Navier-Stokes counterpart, is that the dissipative terms lead to logarithmic divergences in the diagrammatic expansion, and these are resummed to an anomalous exponent. The anomalous exponent can be measured directly in the scaling behavior of the dissipation two-point correlation function, and it also affects the scaling laws of the structure functions. It is shown that when the structure functions exhibit anomalous scaling, the dissipation correlation function does not decay on length scales that are in the scaling range. The implication of our findings is that the concept of an "inertial range" in which the dissipative terms can be ignored is untenable. The consequences of this mechanism for other cases of possible anomalous scaling in turbulence are discussed.

PACS number(s): 47.27.Eq

I. INTRODUCTION

The community of fluid mechanics is split into two camps: one camp believes that the scaling theory of turbulent media is adequately described by the Kolmogorov-Obukhov 1941 phenomenology [1,2] (KO41), whereas the other continues to be troubled by experimental indications that the KO41 predictions are not obeyed (see, for example, Refs. [3-5]). The issue is whether dimensional analysis is sufficient to predict the full scaling behavior of the theory of turbulence. This behavior may be characterized in terms of the structure functions of the hydrodynamic fields. Denoting the velocity field by $\mathbf{u}(\mathbf{x}, t)$ and a generic passive scalar field by $T(\mathbf{x}, t)$, the structure functions are defined in terms of differences across a scale r :

$$S_q(u) \equiv \langle [\delta u_r(\mathbf{x})]^q \rangle \sim r^{q\zeta_q(u)}, \quad (1.1)$$

$$S_q(r) \equiv \langle [\delta T_r(\mathbf{x})]^q \rangle \sim r^{q\zeta_q(T)}, \quad (1.2)$$

where

$$\delta u_r(\mathbf{x}) = [\mathbf{u}(\mathbf{x} + \mathbf{r}) - \mathbf{u}(\mathbf{x})] \cdot \frac{\mathbf{r}}{r}, \quad (1.3)$$

$$\delta T_r(\mathbf{x}) = T(\mathbf{x} + \mathbf{r}) - T(\mathbf{x}). \quad (1.4)$$

Here ζ_q are scaling exponents, and $\langle \dots \rangle$ denotes an average over time. Equations (1.1) and (1.2) are expected to hold over an "inertial range" of scales much smaller than the outer scale of the velocity field L and much larger than a q -dependent integral scale that depends on the Reynolds number $\text{Re} = U_L L / \nu$, with ν being the kinematic viscosity of the fluid and U_L the variation of the velocity field on scale L .

Within the KO41 phenomenology one expects the numerical values of ζ_q to be q independent. For homogeneous isotropic turbulence the prediction [1,2,6,7] is that $\zeta_q(u) = \zeta_q(T) = \zeta = 1/3$. We shall refer to this prediction as "normal scaling." Experiments seem to indicate that this prediction is not obeyed [8]. For higher-order structure functions of the velocity field (high q) there have been claims that significant deviations from normal scaling are observed [5]. Recently also the low values of q were examined using data analysis [9] suggesting that for $q < 3$ the exponents are larger than $1/3$ and for $q > 3$ smaller than $1/3$. (Of course, Cauchy-Schwartz inequalities lead immediately to the constraints $\zeta_q \geq \zeta_{q'}$ for any $q' > q$.)

From the theoretical point of view the situation is even more confusing. There have been many attempts to construct phenomenological models to describe anomalous scaling in turbulence [10,11]. A starting point for some attempts was the observation that the two-point structure function of the dissipation fluctuations depends on the separation distance even when the latter is in the inertial range. The dissipation field in turbulence ϵ has a correlation function which was observed [12] to decay in space like $(L/r)^\mu$. It was erroneously argued (and see below, Sec. VII) that the KO41 theory predicts that $\mu = 0$. The exponent μ was called the "intermittency exponent." Mandelbrot suggested that its nonzero value stems from some fractal concentration of turbulence [13]. Mandelbrot's idea led to a flurry of models [14,15], all of which suffer from a lack of connection to the equations of fluid mechanics. We shall show in this paper that, for the passive scalar field, the exponent of the dissipation correlation function has nothing to do with any fractal

concentration, but that it is important for the understanding of the appearance of multiscaling.

More systematic derivations based on the equations of fluid mechanics have tended to find scaling solutions that agree with the KO41 phenomenology [16,17]. Here we refer to perturbation expansions, whether arbitrarily truncated or fully renormalized. It is noteworthy that the renormalized perturbation approaches have indicated that the expansion converges term by term [17,18]. There seems to be no reason to expect divergences that must be resummed in order to get anomalous exponents. One of the main aims of this paper is to question some of the assertions of these approaches, and to investigate what might be the reason for the failure to find possible mechanisms for anomalous scaling. Following Lebedev and L'vov [19] we shall make the point in this paper that such a mechanism may be furnished by the dissipative terms in the equations of motion.

Rather than dealing directly with all the complications of the Navier-Stokes dynamics, we shall focus here on the scaling behavior of a passive scalar whose dynamics is described by Eq. (2.1). One expects this problem to be simpler, because one can choose the driving velocity field to have a simple scaling behavior, with Gaussian statistics and no multiscaling [i.e., $\zeta_q(u) = \zeta(u)$ for all q]. Some constraints on the possible scaling properties of the passive scalar were established recently using rigorous techniques [20,21]. Two inequalities were derived:

$$2\zeta_1(T) + \zeta(u) \geq 1, \quad (1.5)$$

$$2\zeta_\infty(T) + \zeta(u) \leq 1. \quad (1.6)$$

In the case that the passive scalar has simple scaling, i.e., $\zeta_1(T) = \zeta_\infty(T) = \zeta(T)$, these two inequalities furnish the prediction

$$2\zeta(T) + \zeta(u) = 1 \quad (\text{no anomalous scaling}). \quad (1.7)$$

The rigorous techniques of Refs. [20,21] did not indicate under which conditions one should expect anomalous scaling. Kraichnan has suggested [22] that in the case that the driving velocity field varies on much faster time scales than the passive scalar, Eq. (1.7) will not be obeyed. Kraichnan derived an equation for the two-point correlation function of the passive scalar in this limit [23] and from it computed the value of ζ_2 , finding that this value depends on the dynamical properties of the velocity field. This result means that in this case the two bounds (1.5) and (1.6) may not coincide, and that this case has the potential to exhibit multiscaling. Kraichnan went on to derive an expression for ζ_{2n} under certain assumptions, and found that it has a nontrivial dependence on n .

In this paper we follow Kraichnan's insight [22,23], and perform a systematic study of the scaling solutions of the equation for a passive scalar which is convected by a rapidly varying velocity field. By "rapidly varying" we mean that the typical (k -dependent) frequency scale of the velocity field, Γ_k , is much larger than the typical frequency scale γ_k of the scalar field, so $\gamma_k/\Gamma_k \ll 1$. We will show that the existence of this small parameter allows us to treat the Dyson-Wyld equations [24] of

renormalized perturbation theory in a way that leads to closed form equations. In the limit that $\gamma_k/\Gamma_k \rightarrow 0$ we can solve exactly (in agreement with Kraichnan) for the two-point propagators, whereas the calculation of higher-order correlation functions still involves an infinite series of diagrams. In the investigation of this series we follow the idea presented by Lebedev and L'vov [19] that the diffusive term in the equation of motion is responsible for the appearance of logarithmic divergences in the series, and that these can be resummed exactly, leading to anomalous scaling. We will show within a consistent theory how the possibility of anomalous scaling in the structure functions $S_{2n}(r)$ may arise. It is noteworthy that these divergences do not go away in the limit that the diffusivity goes to zero; we argue that in this problem the notion of an inertial range, in which the diffusive term is negligible, is untenable. Thus, *a theory that sets from the beginning the diffusive term to zero will miss the mechanism for anomalous scaling of the scalar structure functions*. Needless to say, we would like at the end of our calculations to suggest that the same conclusion may hold for the case of the Navier-Stokes equations and the limit $\nu \rightarrow 0$. We defer further discussion of this point to Sec. VIII.

The equation of motion for a passive scalar is

$$(\partial_t + \mathbf{u} \cdot \nabla)T(\mathbf{x}, t) = \kappa \nabla^2 T(\mathbf{x}, t). \quad (1.8)$$

The velocity field $\mathbf{u}(\mathbf{x}, t)$ is externally determined, and we are interested in the effects of this velocity field on the scalar T . From this equation one may obtain an equation of motion for $S_{2n}(r)$ defined in Eq. (1.2), where we have restricted q for our investigation to even integers $2n$. One first derives an equation [22] for $\delta T(\mathbf{x}, \mathbf{x}', t) \equiv T(\mathbf{x}, t) - T(\mathbf{x}', t)$, which is multiplied by $\delta T(\mathbf{x}, \mathbf{x}', t)^{2n-1}$ and averaged over the ensemble to obtain in the stationary case

$$\mathcal{D}_{2n}(r) = J_{2n}(r), \quad (1.9)$$

where, with $r \equiv |\mathbf{x} - \mathbf{x}'|$,

$$\mathcal{D}_{2n}(r) = 2n \langle \delta T^{2n-1}(\mathbf{x}, \mathbf{x}', t) \times [\mathbf{u}(\mathbf{x}, t) \cdot \nabla + \mathbf{u}(\mathbf{x}', t) \cdot \nabla'] \delta T(\mathbf{x}, \mathbf{x}', t) \rangle, \quad (1.10)$$

and

$$J_{2n}(r) = 2n\kappa \langle \delta T^{2n-1}(\mathbf{x}, \mathbf{x}', t) [\nabla^2 + \nabla'^2] \delta T(\mathbf{x}, \mathbf{x}', t) \rangle. \quad (1.11)$$

For future comparison with Kraichnan's derivation [22] of the scaling exponents, we mention here that his analysis is based on the balance equation (1.9), and upon a differential equation which determines the convective term $\mathcal{D}_{2n}(r)$ in terms of the structure function $S_{2n}(r)$ (for general dimension of space d):

$$\mathcal{D}_{2n}(r) = \frac{1}{r^{d-1}} \frac{\partial}{\partial r} \left[r^{d-1} h(r) \frac{\partial S_{2n}(r)}{\partial r} \right]. \quad (1.12)$$

The function $h(r)$ is the "eddy diffusivity" [23],

$$h(\mathbf{r}) = \int_{-\infty}^t dt \langle [\mathbf{u}(\mathbf{x} + \mathbf{r}, t) - \mathbf{u}(\mathbf{x}, t)] \cdot [\mathbf{u}(\mathbf{x} + \mathbf{r}, 0) - \mathbf{u}(\mathbf{x}, 0)] \rangle \quad (1.13)$$

which is assumed to depend on r like $h(r) \sim r^{\zeta_h}$. In our derivation in this paper we will recover this relation for $D_{2n}(r)$. Kraichnan [22] used another relation which is crucial for his results, an approximation for the dissipative term $J_{2n}(r)$:

$$J_{2n}(r) = 2n\kappa S_{2n}(r) [\nabla^2 S_2(r) - \nabla^2 S_2(0)] / S_2(r). \quad (1.14)$$

Our calculation leads to a different evaluation of $J_{2n}(r)$. Using Eqs. (1.10)–(1.14) for $n = 1$, one may determine the coefficients of $S_2(r)$. For general n , one may then use the balance equation, evaluating $D_{2n}(r)$ according to (1.12) and $J_{2n}(r)$ according to (1.14) to derive an equation for the coefficients which determines the scaling exponents. The result [22] is

$$\zeta_{2n}(2n\zeta_{2n} - 2\zeta_2 + d) = d\zeta_2. \quad (1.15)$$

We shall not regain this equation.

A part of the strategy of this paper is to treat the problem in (\mathbf{k}, ω) space instead of the configuration space (\mathbf{r}, t) . Although this is a traditional approach in the analytic theory of turbulence, it needs discussion. After all, plane waves are not the natural representation of one's intuition about turbulent "eddies." It is not obvious that the (\mathbf{k}, ω) representation is efficient in describing the fine scale structures which develop on the viscous scales, and are suspected to play an important role in the theory, as we also claim in this paper. On the other hand, the (\mathbf{k}, ω) representation offers a kit of powerful technical tools. We shall show that in the case that we are considering here we can deal with *all* the important terms in the infinite series of our perturbation theory. We will resum all the diagrams which describe the important role of the viscous-scale structures, and analyze their effect on the fluctuations in the inertial range. Thus, the main complaint about traditional perturbative studies, i.e., that they resort to uncontrolled assumptions about the infinite series of diagrams, will in part be answered in this case.

The structure of this paper is as follows. In Sec. II we develop the line-renormalized perturbation theory for a passive scalar. It has been shown that in order to avoid infrared (ir) divergences due to sweeping effects one may transform to quasi-Lagrangian variables as introduced in Ref. [17], and see also Ref. [18]. This transformation is exact, and it indeed allows us to eliminate the divergences; the price is that we lose momentum conservation at the vertices, and the theory becomes technically more cumbersome. We discuss the renormalized Dyson-Wyld equations in quasi-Lagrangian variables for the case at hand (Sec. II A) and show how the separation of time scales between the velocity field and the passive scalar can be used to effectively eliminate many diagrams from the renormalized expansion. In Sec. III we solve for the two-point Green's function and the correlation function. This solution is exact and leads to a calculation of the

exponent $\zeta_2(T)$. This exponent is not in agreement with (1.7), indicating that the bounds (1.5) and (1.6) do not coincide in this case, and that we should expect multiscaling. We begin to study the mechanism for multiscaling in Sec. IV. We analyze the nonlinear Green's function and find that this quantity is represented by an infinite set of diagrams ("ladder diagrams"), each of which contains a logarithmic divergence in the ultraviolet (uv). Happily, we can resum this set of diagrams exactly, and prove that it leads to an anomalous exponent in the nonlinear Green's function. Sections V and VI are dedicated to understanding how the anomalous exponent found in Sec. IV appears in the scaling properties of the structure functions. To this aim we explore in Sec. V the various higher-order correlation functions and structure functions, and in Sec. VI the quantities J_{2n} . We show that the same ladder diagrams that appear in the nonlinear Green's functions appear as parts of the diagrams for J_{2n} , leading to the appearance of the anomalous exponent also in J_{2n} . We explain how this affects the structure functions in Sec. VI. Section VII deals with the calculation of the two-point correlation function of the scalar dissipation, which is analogous to the correlation of the energy dissipation rate and which also has anomalous scaling behavior of the same nature; see Ref. [19]. It culminates in showing that the anomalous exponent appears once again in the power law decay of this quantity. In fact, it is shown that the borderline of the appearance of multiscaling corresponds in our theory to the elimination of the spatial decay of this correlation function in the scaling regime. This finding is in fact in glaring contradiction with the folklore that ascribes "intermittency corrections" to *deviations* from r^0 behavior of the dissipation correlation. Quite to the contrary, such a behavior is the necessary condition for anomalous scaling in the structure functions. Section VIII is dedicated to a summary and a discussion of this paper. We shall also make in this section some comments about the implications of our analysis on the scaling theory of the structure functions of the velocity field in Navier-Stokes turbulence [25].

II. RENORMALIZED PERTURBATION THEORY FOR A PASSIVE SCALAR

A. Quasi-Lagrangian formulation

Let us return to the equation of motion (1.8) and add an external force $\xi(\mathbf{x}, t)$ which mimics a source of scalar fluctuations with the characteristic scale L :

$$(\partial_t + \mathbf{u} \cdot \nabla)T(\mathbf{x}, t) = \kappa \nabla^2 T(\mathbf{x}, t) + \xi(\mathbf{x}, t). \quad (2.1)$$

The external force $\xi(\mathbf{x}, t)$ is assumed to be Gaussian and statistically homogeneous in space and time. The properties of the correlation function of $\xi(\mathbf{x}, t)$ are best stated in \mathbf{k} space: it is concentrated in the small k region, i.e., $k < 1/L$, and it decays quickly to zero for $k \gg 1/L$. In \mathbf{r}

space this means that $\langle \xi(\mathbf{x}, t) \xi(\mathbf{x} + \mathbf{r}, t) \rangle$ is constant for $r \ll L$.

The perturbation theory of Eq. (2.1) suffers from infrared divergences. It was found in the context of the analysis of the Navier-Stokes equations that these divergences can be removed by transforming the equations to quasi-Lagrangian coordinates [17,18]. This is a useful approach for our problem as well. To perform a quasi-Lagrangian coordinate transformation, all the velocities are taken relative to the velocity of a chosen point which passes through \mathbf{r}_0 at time t_0 . Note that this differs from the Lagrangian transformation where one would follow the trajectory of every point. The quasi-Lagrangian transformation is not an approximation, but a nonlinear transformation of the variables which will allow us to eliminate divergences that are due to larger scale motions. The Euler velocity and the passive scalar fields transform as

$$\mathbf{u}(\mathbf{x}, t) = \mathbf{v}_{\mathbf{r}_0, t_0}(\mathbf{R}, t), \quad (2.2)$$

$$T(\mathbf{x}, t) = \Theta_{\mathbf{r}_0, t_0}(\mathbf{R}, t), \quad (2.3)$$

$$\xi(\mathbf{x}, t) = \phi_{\mathbf{r}_0, t_0}(\mathbf{R}, t), \quad (2.4)$$

where the quasi-Lagrangian trajectory is

$$\mathbf{R}(t) = \mathbf{x} - \int_{t_0}^t d\tau \mathbf{v}_{\mathbf{r}_0, t_0}(\mathbf{r}_0, \tau). \quad (2.5)$$

We can write an equation of motion for $\Theta_{\mathbf{r}_0, t_0}(\mathbf{R}, t)$ using Eq. (2.1), Eqs. (2.2)–(2.5), and the chain rule of differentiation:

$$\begin{aligned} \partial_t \Theta_{\mathbf{r}_0}(\mathbf{R}, t) + [\mathbf{v}_{\mathbf{r}_0}(\mathbf{R}, t) - \mathbf{v}_{\mathbf{r}_0}(\mathbf{r}_0, t)] \cdot \nabla \Theta_{\mathbf{r}_0}(\mathbf{R}, t) \\ = \kappa \nabla^2 \Theta_{\mathbf{r}_0}(\mathbf{R}, t) + \phi_{\mathbf{r}_0}(\mathbf{R}, t). \end{aligned} \quad (2.6)$$

In Eq. (2.6) we have dropped the subscript t_0 . The reason is that the equation is invariant to the choice of the origin of time t_0 , but not to the choice of the position \mathbf{r}_0 . At this point we can replace \mathbf{R} by a dummy space variable \mathbf{x} . Define now the Fourier transform of a function $f(\mathbf{x}, t)$ as

$$f(\mathbf{k}, \omega) = \int d\mathbf{x} dt f(\mathbf{x}, t) \exp[i(\mathbf{k} \cdot \mathbf{x} - \omega t)]. \quad (2.7)$$

After Fourier transforming (2.6) with respect to \mathbf{x} and t , we find the equation of motion

$$\begin{aligned} (\omega + i\kappa k^2) \Theta_{\mathbf{r}_0}(\mathbf{k}, \omega) = 2\pi \int \frac{d\mathbf{k}_1}{(2\pi)^3} \frac{d\mathbf{k}_2}{(2\pi)^3} \frac{d\omega_1}{2\pi} \frac{d\omega_2}{2\pi} \\ \times \mathcal{V}_{\mathbf{r}_0}(\mathbf{k}, \mathbf{k}_1, \mathbf{k}_2) \cdot \mathbf{v}_{\mathbf{r}_0}^*(\mathbf{k}_1, \omega_1) \Theta_{\mathbf{r}_0}^*(\mathbf{k}_2, \omega_2) \delta(\omega + \omega_1 + \omega_2) - i\phi_{\mathbf{r}_0}(\mathbf{k}, \omega), \end{aligned} \quad (2.8)$$

where the quasi-Lagrangian vertex $\mathcal{V}_{\mathbf{r}_0}(\mathbf{k}, \mathbf{k}_1, \mathbf{k}_2)$ is given by

$$\begin{aligned} \mathcal{V}_{\mathbf{r}_0}(\mathbf{k}, \mathbf{k}_1, \mathbf{k}_2) = (2\pi)^3 \mathbf{k}_2 [\delta(\mathbf{k} + \mathbf{k}_1 + \mathbf{k}_2) \\ - e^{-i\mathbf{k}_1 \cdot \mathbf{r}_0} \delta(\mathbf{k} + \mathbf{k}_2)]. \end{aligned} \quad (2.9)$$

Notice that without the second term in Eq. (2.9) we recover the Eulerian vertex. With the second term the vertex has useful properties when one of the triad \mathbf{k} vectors is much smaller than the other two. Consider for simplicity the case $\mathbf{r}_0 = \mathbf{0}$ (which is not essential for the argument as is clarified below).

(i) for $|\mathbf{k}| \ll |\mathbf{k}_1|, |\mathbf{k}_2|$,

$$\mathcal{V}_{\mathbf{r}_0}(\mathbf{k}, \mathbf{k}_1, \mathbf{k}_2) = \mathbf{k} \delta(\mathbf{k} + \mathbf{k}_1 + \mathbf{k}_2). \quad (2.10)$$

To see this, notice that by incompressibility we can add a \mathbf{k}_1 to the \mathbf{k}_2 that multiplies the δ functions in Eq. (2.9). Then, using the first δ function we get the result (2.10). The second δ function vanishes in this limit.

(ii) for $|\mathbf{k}_1| \ll |\mathbf{k}|, |\mathbf{k}_2|$,

$$\mathcal{V}_{\mathbf{r}_0}(\mathbf{k}, \mathbf{k}_1, \mathbf{k}_2) = \mathbf{k}_2 \left(\mathbf{k}_1 \cdot \frac{d}{d\mathbf{k}_1} \delta(\mathbf{k} + \mathbf{k}_2) \right). \quad (2.11)$$

The important thing is that the vertex is proportional to \mathbf{k}_1 . This is very different from the Eulerian vertex which

is proportional to \mathbf{k}_2 and consequently much larger than $\mathcal{V}_{\mathbf{r}_0}$.

(iii) for $|\mathbf{k}_2| \ll |\mathbf{k}|, |\mathbf{k}_1|$,

$$\mathcal{V}_{\mathbf{r}_0}(\mathbf{k}, \mathbf{k}_1, \mathbf{k}_2) \propto \mathbf{k}_2, \quad (2.12)$$

as one sees from Eq. (2.9). We conclude that in all these three cases the vertex is proportional to the smallest wave vector. This is the main reason for the quasi-Lagrangian formulation; a similar result for the dynamics of the velocity field under the Navier-Stokes equations has been previously established [17]. This property serves to eliminate divergences that exist in the Eulerian case. We stress that in our derivation below we use the full and exact form of the vertex (2.9). The preceding discussion of the asymptotic properties of the vertex serves only to motivate our choice of coordinates.

We wish to calculate the simultaneous two-point and higher-order correlation functions of the $T(\mathbf{x}, t)$ field. We will use the above equation to calculate the correlation functions of the $\Theta_{\mathbf{r}_0}$ field. It will be clear (see also [17,18]) from the following argument that the simultaneous correlation functions of $T(\mathbf{x}, t)$ coincide with those of $\Theta_{\mathbf{r}_0}$. Since the equations of motion for both T and $\Theta_{\mathbf{r}_0}$ are invariant to translation of the origin of time, simultaneous correlation functions cannot depend explicitly on time. Accordingly one can compute the correlation of $\Theta_{\mathbf{r}_0}$ at

$t = t_0$. At this time the quasi-Lagrangian transformation Eqs. (2.2)–(2.5) is an identity, and the two fields T and $\Theta_{\mathbf{r}_0}$ are identical.

The theory is developed in terms of three two-point propagators, i.e., the correlation function and the Green's function of the passive scalar field $\Theta_{\mathbf{r}_0}$ and the correlation function of the quasi-Lagrangian velocity field $\mathbf{v}_{\mathbf{r}_0}$. These are defined as follows:

$$2\pi\mathcal{F}_{\mathbf{r}_0}(\mathbf{k}_1, \mathbf{k}_2, \omega_1)\delta(\omega_1 + \omega_2) = \langle \Theta_{\mathbf{r}_0}(\mathbf{k}_1, \omega_1)\Theta_{\mathbf{r}_0}(\mathbf{k}_2, \omega_2) \rangle, \quad (2.13)$$

$$2\pi\mathcal{G}_{\mathbf{r}_0}(\mathbf{k}_1, \mathbf{k}_2, \omega_1)\delta(\omega_1 + \omega_2) = \langle \delta\Theta_{\mathbf{r}_0}(\mathbf{k}_1, \omega_1)/\delta\phi^*(\mathbf{k}_2, \omega_2) \rangle, \quad (2.14)$$

$$2\pi\mathcal{H}_{\mathbf{r}_0}(\mathbf{k}_1, \mathbf{k}_2, \omega_1)\delta(\omega_1 + \omega_2) = \langle \mathbf{v}_{\mathbf{r}_0}(\mathbf{k}_1, \omega_1)\mathbf{v}_{\mathbf{r}_0}(\mathbf{k}_2, \omega_2) \rangle. \quad (2.15)$$

These quantities are not diagonal in \mathbf{k} representation because of the existence of the reference point \mathbf{r}_0 . However, the original problem is homogeneous in space. As is shown in Appendix A, this leads to a transformation rule with respect to a change of reference point by \mathbf{R} . This rule [cf. (A9)] is

$$\mathcal{F}_{\mathbf{r}_0-\mathbf{R}}(\mathbf{k}_1, \mathbf{k}_2, \omega_1) = \mathcal{F}_{\mathbf{r}_0}(\mathbf{k}_1, \mathbf{k}_2, \omega_1)e^{-i(\mathbf{k}_1+\mathbf{k}_2)\cdot\mathbf{R}}.$$

This rule can be represented in a simple form in a mixed (\mathbf{k}, \mathbf{r}) representation, where $\mathbf{k} = (\mathbf{k}_1 - \mathbf{k}_2)/2$ and \mathbf{r} is a space coordinate conjugate to $\mathbf{s} = \mathbf{k}_1 + \mathbf{k}_2$. Defining

$$\mathcal{F}_{\mathbf{r}_0}(\mathbf{k}, \mathbf{r}, \omega_1) = \int ds \exp(is \cdot \mathbf{r})\mathcal{F}_{\mathbf{r}_0}(\mathbf{k} + \mathbf{s}/2, -\mathbf{k} + \mathbf{s}/2, \omega_1), \quad (2.16)$$

one may rewrite Eq. (A9) as

$$\mathcal{F}_{\mathbf{r}_0}(\mathbf{k}, \mathbf{r}, \omega_1) = \mathcal{F}(\mathbf{k}, \mathbf{r} - \mathbf{r}_0, \omega_1), \quad (2.17)$$

where we have denoted $\mathcal{F}_{\mathbf{r}_0=0}$ by \mathcal{F} . Similarly, one can derive a corresponding relation for the Green's function. The implication of these relations is that, rather than having a dependence on \mathbf{k}_1 , \mathbf{k}_2 , and \mathbf{r}_0 , the two-point propagators depend on two quantities only, i.e., \mathbf{k} and $\mathbf{r} - \mathbf{r}_0$. The transformation rule Eq. (2.17) demonstrates explicitly that the choice of the reference point \mathbf{r}_0 is identical to a choice of the coordinate origin due to the dependence of the propagators only on the spatial difference $\mathbf{r} - \mathbf{r}_0$. Accordingly, without loss of generality we can choose from now on $\mathbf{r}_0 = \mathbf{0}$ and write the theory in terms of the quantities $\mathcal{F}(\mathbf{k}, \mathbf{r}, \omega_1)$, $\mathcal{G}(\mathbf{k}, \mathbf{r}, \omega_1)$ or their Fourier transforms with respect to \mathbf{r} .

Since the velocity field in our problem is at our disposal, we shall introduce a physical model that simplifies

the calculations. From the point of view of Navier-Stokes dynamics, a “fast-varying” velocity field is only realizable when the nonlinear term in the equations is negligible, and the dynamics is dominated by the external forcing which is fast varying. When the nonlinearity is small, there is no appreciable difference between Eulerian and quasi-Lagrangian coordinates. We can therefore take the following form for $\mathcal{H}_{\mathbf{r}_0}(\mathbf{k}_1, \mathbf{k}_2, \omega_1)$:

$$\mathcal{H}_{\mathbf{r}_0}(\mathbf{k}_1, \mathbf{k}_2, \omega_1) = \mathbf{P}_{\mathbf{k}_1}\mathcal{H}(k_1)f\left(\frac{\omega_1}{\Gamma_{k_1}}\right)\delta(\mathbf{k}_1 + \mathbf{k}_2), \quad (2.18)$$

where $f(\omega_1/\Gamma_k)$ is a scaling function, $\int dx f(x) = 1$, and $f(0) = O(1)$. $\mathbf{P}_{\mathbf{k}}$ is the transverse projection operator

$$\mathbf{P}_{\mathbf{k}}^{\alpha\beta} = \delta_{\alpha\beta} - \frac{k^\alpha k^\beta}{k^2}, \quad (2.19)$$

and

$$\mathcal{H}(k) = \frac{H(k)}{\Gamma_k} \sim \frac{H}{k^x}. \quad (2.20)$$

The quantity Γ_k is the characteristic frequency of variation of the quasi-Lagrangian (and Lagrangian) velocity field on a scale $1/k$. We are interested in this paper in the case where Γ_k is large, in a sense to be made precise later.

B. Dyson-Wyld equations

In this subsection we develop a line-renormalized perturbation theory for the two-point propagators. We choose graphic notation as shown in Fig. 1.

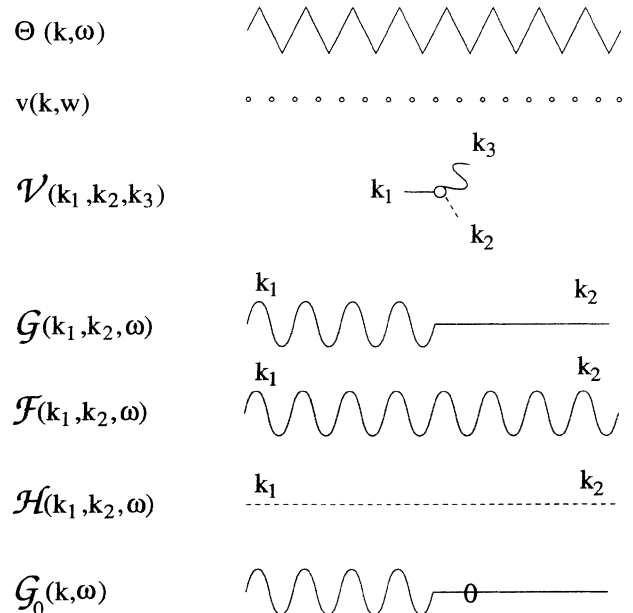


FIG. 1. Notation.

In Fig. 2 we show the diagrammatic representation of the equation of motion (2.8) in terms of renormalized propagators. Despite the fact that our propagators (and our vertex) are not diagonal in \mathbf{k} representation, one can perform the standard Dyson summation of the one-particle irreducible diagrams to obtain the well-known Dyson-Wyld equations. With our notation the Dyson-Wyld equations are shown in Fig. 3, where we also display the first contributions to the mass operators Σ (renormalized damping) and Φ (renormalized noise correlations). In analytic form the Dyson equation for the Green's function and the Wyld equation for the correlation function read

$$\mathcal{G}(\mathbf{k}_1, \mathbf{k}_2, \omega_1) = \mathcal{G}_0(\mathbf{k}_1, \omega_1) \left[(2\pi)^3 \delta(\mathbf{k}_1 + \mathbf{k}_2) - \int \frac{d\mathbf{k}_3}{(2\pi)^3} \Sigma(\mathbf{k}_1, \mathbf{k}_3, \omega_1) \mathcal{G}(\mathbf{k}_3, \mathbf{k}_2, \omega_1) \right], \quad (2.21)$$

$$\mathcal{F}(\mathbf{k}_1, \mathbf{k}_2, \omega_1) = \int \frac{d\mathbf{k}_3}{(2\pi)^3} \frac{d\mathbf{k}_4}{(2\pi)^3} \times \mathcal{G}(\mathbf{k}_1, \mathbf{k}_3, \omega_1) \Phi(\mathbf{k}_3, \mathbf{k}_4, \omega_1) \times \mathcal{G}^*(\mathbf{k}_2, \mathbf{k}_4, \omega_1), \quad (2.22)$$

where the bare Green's function is $\mathcal{G}_0(\mathbf{k}, \omega) = (\omega + i\kappa k^2)^{-1}$.

In order to solve these equations we need to examine the series for Σ and Φ . The lowest-order contributions for these are

$$\Sigma^{(2)}(\mathbf{k}_1, \mathbf{k}_2, \omega) = \int \prod_{j=1}^3 \frac{d\mathbf{p}_j}{(2\pi)^3} \frac{d\omega_1}{2\pi} \mathcal{V}(\mathbf{k}_1, \mathbf{p}_3, \mathbf{p}_1) \cdot \mathcal{H}(\mathbf{p}_3, \omega - \omega_1) \cdot \mathcal{V}(\mathbf{p}_2, \mathbf{p}_3, \mathbf{k}_2) \times \mathcal{G}(\mathbf{p}_1, \mathbf{p}_2, \omega_1), \quad (2.23)$$

$$\Phi^{(2)}(\mathbf{k}_1, \mathbf{k}_2, \omega) = \int \prod_{j=1}^3 \frac{d\mathbf{p}_j}{(2\pi)^3} \frac{d\omega_1}{2\pi} \mathcal{V}(\mathbf{k}_1, \mathbf{p}_3, \mathbf{p}_1) \cdot \mathcal{H}(\mathbf{p}_3, \omega - \omega_1) \cdot \mathcal{V}(\mathbf{k}_2, \mathbf{p}_3, \mathbf{p}_2) \times \mathcal{F}(\mathbf{p}_1, \mathbf{p}_2, \omega_1), \quad (2.24)$$

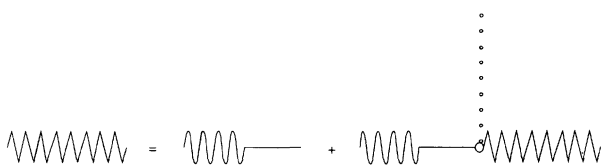


FIG. 2. Equation of motion for Θ .

Dyson Equation

$$(a) \quad \text{wavy line} = \text{wavy line} + \text{wavy line} \circlearrowleft (\Sigma) \text{wavy line}$$

Wyld Equation

$$(b) \quad \text{wavy line} = \text{wavy line} \circlearrowleft (\Phi) \text{wavy line}$$

where

$$(c) \quad \text{circle with } \Sigma = \text{diagram 1} + \text{diagram 2} + \dots$$

$$(d) \quad \text{circle with } \Phi = \text{diagram 1} + \text{diagram 2} + \dots$$

$$(e) \quad \text{diagram with time labels } t_1, t_2$$

FIG. 3. Dyson-Wyld equations.

where Eq. (2.18) has been used. We will show now that for the problem at hand all the higher-order contributions to Σ and Φ are negligible, and vanish in the limit of an infinitely fast-varying velocity field. Accordingly, Eqs. (2.23) and (2.22) close the Dyson-Wyld equations. A similar situation occurs in the problem of weak localization [26].

To see why all the other diagrams vanish in the limit it is useful to consider the diagrams in the time domain rather than in the frequency domain. Every propagator propagates from a time t_1 to a time t_2 . The Green's functions are time ordered; due to causality $G(\mathbf{k}_1, \mathbf{k}_2, t_1, t_2)$ vanishes for $t_1 < t_2$. The velocity correlator, in the limit of extremely fast decay, can be thought of as a δ function in time, $\delta(t_1 - t_2)$. Consider the second diagram in Fig. 3(c), which is redrawn with time labels in Fig. 3(e). Due to causality it must vanish, since t_2 has to be both smaller and larger than t_1 . The key feature is that all the diagrams except the first contain interlocked dashed lines of the velocity correlator and this will always violate causality. The series consists entirely of such diagrams because these are all irreducible contributions; the uninterlocked diagrams have been resummed already into the definition of the renormalized (i.e., dressed) propagators.

If the correlator is not quite a δ function, we gain a factor of $(\gamma/\Gamma)^2$ in this diagram. Higher-order diagrams have even higher powers of this small parameter, and will all vanish in the limit $\gamma/\Gamma \rightarrow 0$.

In order to demonstrate this explicitly, Appendix B contains a calculation of the next-order diagram in the one-pole approximation, which reveals a coefficient of γ/Γ .

III. THE TWO-POINT PROPAGATORS OF THE PASSIVE SCALAR

In this section we analyze the Dyson-Wyld equations (2.21)–(2.24) with the aim of understanding the properties of the two-point propagators $\mathcal{G}(\mathbf{k}_1, \mathbf{k}_2, \omega)$ and $\mathcal{F}(\mathbf{k}_1, \mathbf{k}_2, \omega)$ of the scalar field.

A. The properties of the Green's function

Consider first Eq. (2.23). For Γ_k very large, we can evaluate \mathcal{H} in the limit $\omega = 0$, where the scaling function $f(0) = O(1)$. Therefore the frequency integration in the loop is over the Green's function $\mathcal{G}(\mathbf{k}_3, \mathbf{k}_4, \omega_1)$ only. This integration leads to $\mathcal{G}(\mathbf{k}_3, \mathbf{k}_4, t = 0)$. For $t = 0$ the Eulerian and quasi-Lagrangian Green's functions coincide. Accordingly, $\mathcal{G}(\mathbf{k}_1, \mathbf{k}_2, t = 0) = (2\pi)^3 \mathcal{G}_E(\mathbf{k}_1, t = 0) \delta(\mathbf{k}_1 + \mathbf{k}_2)$. The Eulerian Green's function \mathcal{G}_E satisfies the sum rule

$$\int d\omega \mathcal{G}_E(\mathbf{k}, \omega) = -i\pi, \quad (3.1)$$

and therefore

$$\int \frac{d\omega}{2\pi} \mathcal{G}(\mathbf{k}_1, \mathbf{k}_2, \omega) = -\frac{i}{2} (2\pi)^3 \delta(\mathbf{k}_1 + \mathbf{k}_2). \quad (3.2)$$

Using this form in Eq. (2.23) we find that $\Sigma^{(2)}$ becomes frequency independent and may be written as

$$\begin{aligned} \Sigma^{(2)}(\mathbf{k}_1, \mathbf{k}_2) &= -\frac{i}{2} \int dp dq (\mathbf{p} \cdot \mathbf{P}_q \cdot \mathbf{k}_2) \mathcal{H}(q) \\ &\quad \times [\delta(\mathbf{k}_1 + \mathbf{p} + \mathbf{q}) - \delta(\mathbf{k}_1 + \mathbf{p})] \\ &\quad \times [\delta(\mathbf{k}_2 + \mathbf{p} + \mathbf{q}) - \delta(\mathbf{k}_2 + \mathbf{p})], \end{aligned}$$

where we have replaced $\mathcal{H}(\mathbf{q}, \omega)$, as explained, by $\mathbf{P}_q \mathcal{H}(q)$. The result of the calculation is

$$\begin{aligned} \Sigma^{(2)}(\mathbf{k}_1, \mathbf{k}_2) &= -i \left[\frac{2}{3} \mathbf{k}_1 \cdot \mathbf{k}_2 \delta(\mathbf{k}_1 + \mathbf{k}_2) \int dq \mathcal{H}(q) \right. \\ &\quad \left. - (\mathbf{k}_1 \cdot \mathbf{P}_{12} \cdot \mathbf{k}_2) \mathcal{H}(|\mathbf{k}_1 + \mathbf{k}_2|) \right], \quad (3.3) \end{aligned}$$

where $\mathbf{P}_{12} \equiv \mathbf{P}_{\mathbf{k}_1 + \mathbf{k}_2}$. Note that $\Sigma^{(2)}(\mathbf{k}_1, \mathbf{k}_2) = \Sigma^{(2)}(\mathbf{k}_2, \mathbf{k}_1)$. Since we have already argued that all the higher-order contributions to Σ vanish in the limit $\Gamma \rightarrow \infty$, we can substitute $\Sigma^{(2)}$ into Eq. (2.21) to derive a closed integral equation for the Green's function:

$$\begin{aligned} \omega \mathcal{G}(\mathbf{k}_1, \mathbf{k}_2, \omega) &= (2\pi)^3 \delta(\mathbf{k}_1 + \mathbf{k}_2) \\ &\quad + i(2\pi)^3 \int \frac{dq}{(2\pi)^3} (\mathbf{k}_1 \cdot \mathbf{P}_q \cdot \mathbf{k}_1) \mathcal{H}(q) \\ &\quad \times [\mathcal{G}(\mathbf{k}_1 + \mathbf{q}, \mathbf{k}_2, \omega) - \mathcal{G}(\mathbf{k}_1, \mathbf{k}_2, \omega)]. \quad (3.4) \end{aligned}$$

In writing Eq. (3.4) we have approximated \mathcal{G}_0^{-1} as ω , neglecting κk^2 . Although the neglect of κk^2 is a usual procedure for k in the ‘‘inertial range,’’ we will have to return to a careful discussion of this step at a later stage of the

calculation; see Sec. VIII. An important point to notice is that without the second Green's function that originates from the quasi-Lagrangian transformation the integral in (3.4) may not be bounded at its lower limit. This infrared divergence is the reason for the introduction of the quasi-Lagrangian coordinates. We shall see that this divergence is eliminated in the present formulation. Furthermore, we show in Appendix C that $\mathcal{G}(\mathbf{k}_1, \mathbf{k}_2, \omega)$ is symmetric under exchange of \mathbf{k}_1 and \mathbf{k}_2 .

Let us now integrate out the second argument of the Green's function to obtain an equation for the function $G(\mathbf{k}, \omega)$,

$$G(\mathbf{k}, \omega) - \int \frac{d\mathbf{k}_1}{(2\pi)^3} \mathcal{G}(\mathbf{k}, \mathbf{k}_1, \omega). \quad (3.5)$$

This equation then reads

$$\begin{aligned} \omega G(\mathbf{k}, \omega) &= 1 + ik^2 \int \frac{dq}{(2\pi)^3} \sin^2 \theta_{kq} \mathcal{H}(q) \\ &\quad \times [G(\mathbf{k} + \mathbf{q}, \omega) - G(\mathbf{k}, \omega)], \quad (3.6) \end{aligned}$$

where θ_{kq} is the angle between \mathbf{k} and \mathbf{q} . For \mathcal{H} going as $1/q^x$, it can be seen from this equation that there are no infrared divergences in this integral for $3 < x < 5$. Since $\mathcal{H}(q)$ decays sufficiently rapidly for large q , the main contribution to the integral comes from the region $q \simeq k$. Introduce therefore a scaling form for $G(\mathbf{k}, \omega)$,

$$G(\mathbf{k}, \omega) = \frac{1}{\gamma_k} g\left(\frac{\omega}{\gamma_k}\right), \quad \gamma_k = \gamma k^z, \quad (3.7)$$

and by power counting find the scaling relation

$$z + x = 5. \quad (3.8)$$

Note that in this case the dynamic exponent z is determined completely by the static exponent x of the velocity field.

Finally, in Appendix D, the asymptotic properties of the Green's function at large frequencies are derived. It is shown that the real part behaves like $1/\omega$, and the imaginary part is proportional to $1/\omega^{(1+2/z)}$.

B. The properties of the correlation function

In this section we shall find the scaling exponent of the simultaneous correlation function of the scalar field that will be denoted as $F(\mathbf{k})$. This quantity is obtained from $\mathcal{F}(\mathbf{k}_1, \mathbf{k}_2, \omega_1)$ by integrating $d\omega_1/2\pi$. After integration we have the simultaneous quantity, which is the same as the Eulerian quantity, denoted by $F(k)$. We shall assume a scaling form for $F(k)$,

$$F(k) = \frac{F}{k^y}. \quad (3.9)$$

We begin by using Eq. (2.24) to rewrite Φ in explicit form:

$$\begin{aligned} \Phi^{(2)}(\mathbf{k}_1, \mathbf{k}_2, \omega) &= \int \prod_{j=1}^3 \frac{d\mathbf{p}_j}{(2\pi)^3} \frac{d\omega_1}{2\pi} \\ &\quad \times \mathcal{H}(\mathbf{p}_3) (\mathbf{p}_1 \cdot \mathbf{P}_3 \cdot \mathbf{p}_2) \mathcal{F}(\mathbf{p}_1, \mathbf{p}_2, \omega_1) \\ &\quad \times (2\pi)^6 [\delta(\mathbf{k}_1 + \mathbf{p}_1 + \mathbf{p}_3) - \delta(\mathbf{k}_1 + \mathbf{p}_1)] \\ &\quad \times [\delta(\mathbf{k}_2 + \mathbf{p}_2 + \mathbf{p}_3) - \delta(\mathbf{k}_2 + \mathbf{p}_2)], \quad (3.10) \end{aligned}$$

where we have replaced \mathcal{H} by the projection operator form as done in Sec. III A and displayed the form of the vertices. Performing the integration over ω_1 and using the same arguments about the $t = 0$ value of the correlation function as in Sec. III A we find

$$\begin{aligned} \Phi^{(2)}(\mathbf{k}_1, \mathbf{k}_2, \omega) &= \int d\mathbf{p}d\mathbf{q} \mathcal{H}(q)(\mathbf{p} \cdot \mathbf{P}_q \cdot \mathbf{p})F(\mathbf{p}) \\ &\quad \times [\delta(\mathbf{k}_1 + \mathbf{p} + \mathbf{q}) - \delta(\mathbf{k}_1 + \mathbf{p})] \\ &\quad \times [\delta(\mathbf{k}_2 + \mathbf{p} + \mathbf{q}) - \delta(\mathbf{k}_2 + \mathbf{p})]. \end{aligned} \quad (3.11)$$

From this expression it is clear that $\Phi^{(2)}$ is symmetric in $\mathbf{k}_1, \mathbf{k}_2$ and is frequency independent.

In order to determine the scaling exponents for the correlation function we proceed now to arrive at a useful form of the Dyson-Wyld equations. In Appendix E we show that the Dyson equation for the imaginary part of the Green's function \mathcal{G}'' may be written as

$$\mathcal{G}''_{12} = \mathcal{G}_{13}\Sigma''_{34}\mathcal{G}^*_{24}, \quad (3.12)$$

where we introduce the matrix notation $\mathcal{G}_{12} = \mathcal{G}(\mathbf{k}_1, \mathbf{k}_2, \omega)$ and the implied summation represents an integration over the indexed variable. The Wyld equation is rewritten in this notation as

$$\mathcal{F}_{12} = \mathcal{G}_{13}\Phi_{34}\mathcal{G}^*_{42}. \quad (3.13)$$

Because of the symmetry of \mathcal{G} , $\mathcal{G}^*_{42} = \mathcal{G}^*_{24}$, we can rewrite the last two equations in condensed matrix notation where we abbreviate the above summation by the symbol $*$:

$$\mathcal{F} = \mathcal{G} * \Phi * \mathcal{G}^*, \quad (3.14)$$

$$\mathcal{G}'' = \mathcal{G} * \Sigma'' * \mathcal{G}^*. \quad (3.15)$$

Multiplying both equations on the left by \mathcal{G}^{-1} and respectively by Σ'' and Φ we find

$$\mathcal{G}^{-1} * \mathcal{F} * \Sigma'' = \Phi * \mathcal{G}^* * \Sigma'', \quad (3.16)$$

$$\mathcal{G}^{-1} * \mathcal{G}'' * \Phi = \Sigma'' * \mathcal{G}^* * \Phi = \Phi * \mathcal{G}^* * \Sigma'', \quad (3.17)$$

where in the last step we have used the symmetry properties of all the functions. Subtracting Eq. (3.17) from Eq. (3.16) we obtain

$$\mathcal{F} * \Sigma'' = \mathcal{G}'' * \Phi. \quad (3.18)$$

This equation can also be written as

$$\text{Im} [\Sigma_{13}\mathcal{F}_{32} + \Phi_{13}\mathcal{G}^*_{32}(\omega)] = 0. \quad (3.19)$$

Integrating over frequencies and using the identity of the $t = 0$ quasi-Lagrangian and Eulerian propagators, we finally conclude that

$$\Sigma''(\mathbf{k}_1, \mathbf{k}_2)F(\mathbf{k}_2) + \frac{1}{2}\Phi(\mathbf{k}_1, \mathbf{k}_2) = 0. \quad (3.20)$$

Similarly one can derive

$$\Sigma''(\mathbf{k}_1, \mathbf{k}_2)F(\mathbf{k}_1) + \frac{1}{2}\Phi(\mathbf{k}_1, \mathbf{k}_2) = 0. \quad (3.21)$$

Adding the last two equations together, and using the forms of Σ and Φ , we find

$$\begin{aligned} &\Phi(\mathbf{k}_1, \mathbf{k}_2) + \Sigma''(\mathbf{k}_1, \mathbf{k}_2)[F(\mathbf{k}_1) + F(\mathbf{k}_2)] \\ &= \int d\mathbf{p}d\mathbf{q} \mathcal{H}(q)(\mathbf{p} \cdot \mathbf{P}_q \cdot \mathbf{p})[2F(\mathbf{p}) - F(\mathbf{k}_1) - F(\mathbf{k}_2)] \\ &\quad \times [\delta(\mathbf{k}_1 + \mathbf{p} + \mathbf{q}) - \delta(\mathbf{k}_1 + \mathbf{p})] \\ &\quad \times [\delta(\mathbf{k}_2 + \mathbf{p} + \mathbf{q}) - \delta(\mathbf{k}_2 + \mathbf{p})] = 0. \end{aligned} \quad (3.22)$$

This simplifies to the diagonal form

$$\begin{aligned} &\int d\mathbf{p}d\mathbf{q} \mathcal{H}(q)\delta(\mathbf{k} + \mathbf{p} + \mathbf{q})(\mathbf{p} \cdot \mathbf{P}_q \cdot \mathbf{p}) \\ &\quad \times [F(\mathbf{p}) - F(\mathbf{k})]\delta(\mathbf{k}_1 + \mathbf{k}_2) = 0. \end{aligned} \quad (3.23)$$

This equation will enable us to obtain the scaling exponent of $F(k)$. In order to do this, denote the function in front of $\delta(\mathbf{k}_1 + \mathbf{k}_2)$ on the left-hand side (LHS) of Eq. (3.23) as L_k . Next write $L_k = \frac{1}{2}(L_k + L_k)$. In the second L_k we will use a transformation of the integrand that was introduced in Refs. [27–29]. Define an operator \mathcal{R}_λ on the space of vectors according to the requirement that

$$\mathbf{k} = \mathcal{R}_\lambda \mathbf{p}. \quad (3.24)$$

This operator rotates by the angle between \mathbf{k} and \mathbf{p} , and dilates by the factor $\lambda = k/p$. Introduce the new variables

$$\mathbf{p}' = \mathcal{R}_\lambda \mathbf{k} = \mathcal{R}_\lambda \mathcal{R}_\lambda \mathbf{p}, \quad (3.25)$$

$$\mathbf{q}' = -\mathcal{R}_\lambda \mathbf{q}, \quad (3.26)$$

$$\mathbf{k}' = \mathcal{R}_\lambda \mathbf{p} = \mathbf{k}. \quad (3.27)$$

Writing then Eq. (3.23) in terms of primed variables ($\mathbf{k} \rightarrow \mathbf{k}'$, $\mathbf{p} \rightarrow \mathbf{p}'$, $\mathbf{q} \rightarrow \mathbf{q}'$) and then using Eqs. (3.25)–(3.27), assuming that the integral converges in the ir and uv regimes, we find that the integral is multiplied by a factor of λ^{8-y-x} , and in the integrand \mathbf{k} and \mathbf{p} exchange positions and $\mathbf{q} \rightarrow -\mathbf{q}$. Thus we have derived the equation

$$\begin{aligned} 0 = L_k &= \int d\mathbf{p}d\mathbf{q} \mathcal{H}(q)\delta(\mathbf{k} + \mathbf{p} + \mathbf{q})(\mathbf{p} \cdot \mathbf{P}_q \cdot \mathbf{p}) \\ &\quad \times [F(\mathbf{p}) - F(\mathbf{k})] \left[1 - \left(\frac{k}{p} \right)^{8-y-x} \right]. \end{aligned} \quad (3.28)$$

Obviously the solution is

$$y = 8 - x, \quad (3.29)$$

which is the desired equation for the scaling exponents. In the Introduction we have defined the scaling exponents ζ_2 and ζ_h as defined by Kraichnan. These exponents are related to x and y according to

$$\zeta_h = x - 3, \quad 2\zeta_2 = y - 3. \quad (3.30)$$

In terms of these scaling exponents the relation (3.29) reads

$$2\zeta_2 = 2 - \zeta_h, \tag{3.31}$$

which is in agreement with Kraichnan's calculation. The reason for this agreement is that (3.29) basically reflects the condition of the constancy of flux of T^2 . We shall see that this agreement is not repeated with ζ_{2n} as there is no such constraint on higher-order quantities T^{2n} . We will explain in detail in Sec. VI why the higher-order fluxes are not constant.

In order to consider the effect of the neglect of the κk^2 terms, one may return to Eq. (3.28) and include the corrections due to diffusion. One may easily determine that this results in corrections to scaling of lower order than the scaling index of \mathcal{F} determined by Eq. (3.29).

Finally, note that the assumption of convergence of the integrals in the ir and the uv prescribes the range of validity $3 \leq x \leq 5$, or $0 \leq \zeta_h \leq 2$, or $0 \leq \zeta_2 \leq 1$, which is the natural range of validity for a scaling (Hölder) exponent.

IV. THE NONLINEAR GREEN'S FUNCTION AND THE MECHANISM FOR ANOMALOUS SCALING

We found that the scaling exponent ζ_2 need not satisfy Eq. (1.7), meaning that the bounds (1.5) and (1.6) may not coincide. We face, therefore, a situation where ζ_1 may differ from ζ_∞ , which is the situation referred to as anomalous scaling. The theory that we develop here does not lend itself easily to the estimation of ζ_1 . It is more natural to study the scaling exponents ζ_{2n} in order to discuss anomalous scaling. We are forced to study higher-order correlations and structure functions whose perturbative expansions do not simplify to one diagram as we have had so far, but rather have an infinity of relevant diagrams. Notwithstanding, if all these diagrams converge in the ir and the uv, we do not have a mechanism for anomalous scaling. Scaling relations that can be found with the lowest-order diagrams persist to all orders if the diagrams are local in \mathbf{k} and ω . (Note that the locality in frequency is proven in Appendix D.) We expect therefore to find divergences in the diagrammatic expansions, and our hope is that these divergences can be resummed to an anomalous exponent. It turns out that there exists one quantity, the nonlinear Green's function, whose diagrammatic expansion offers the cleanest demonstration of the mechanism for anomalous scaling. Furthermore, it provides us with a means to calculate the value of the anomalous exponent from first principles. We therefore focus on this quantity in this section, and learn how to deal with the type of divergences that are going to reappear later in other quantities of interest.

A. The nonlinear Dyson equation

The nonlinear Green's function is defined as

$$2\pi \mathcal{G}_{NL}(\mathbf{k}_1, \mathbf{k}_2, \mathbf{k}_3, \mathbf{k}_4, \omega_1, \omega_2, \omega_3, \omega_4) \delta \left(\sum_{j=1}^4 \omega_j \right) = \langle \langle [\delta\theta(\mathbf{k}_1, \omega_1) / \delta\phi^*(\mathbf{k}_3, \omega_3)] [\delta\theta(\mathbf{k}_2, \omega_2) / \delta\phi^*(\mathbf{k}_4, \omega_4)] \rangle \rangle. \tag{4.1}$$

The diagrammatic series for \mathcal{G}_{NL} is displayed in Fig. 4(a). As in the arguments of Sec. III all the diagrams in which the velocity correlation dashed line is not vertical are negligible in the limit $(\gamma/\Gamma) \rightarrow 0$. The contributing diagrams are the reducible part and the infinite set of "ladder diagrams," whose first two members are shown in Fig. 4(a). This set of ladder diagrams can be resummed straightforwardly to provide the closed form equation for the nonlinear Green's function shown in Fig. 4(b).

For our purposes we need only partial information about \mathcal{G}_{NL} , i.e.,

$$\mathcal{G}_{NL}(\mathbf{k}_1, \mathbf{k}_2, \mathbf{k}_3, \mathbf{k}_4, \Omega) = \int \frac{d\omega_1}{2\pi} \frac{d\omega_3}{2\pi} \mathcal{G}_{NL}(\mathbf{k}_1, \mathbf{k}_2, \mathbf{k}_3, \mathbf{k}_4, \omega_1, \Omega - \omega_1, \omega_3, \Omega - \omega_3). \tag{4.2}$$

This quantity is the Fourier transform of the time-domain function

$$\mathcal{G}_{NL}(\mathbf{k}_1, \mathbf{k}_2, \mathbf{k}_3, \mathbf{k}_4, \tau) = \langle \langle [\delta\theta(\mathbf{k}_1, t + \tau) / \delta\phi^*(\mathbf{k}_3, t)] [\delta\theta(\mathbf{k}_2, t + \tau) / \delta\phi^*(\mathbf{k}_4, t)] \rangle \rangle. \tag{4.3}$$

The resummed series for this quantity is shown in Fig. 5.

B. The mechanism for the anomalous exponent

Consider the nonlinear Green's function in the limit $k_1, k_2 \gg k_3, k_4$. Examine a typical diagram in the expansion of \mathcal{G}_{NL} , such as in Fig. 6. Let us take for the purposes of calculation the Green's function to have the Eulerian property

$$\mathcal{G}(\mathbf{k}_1, \mathbf{k}_2, \omega) = G(\mathbf{k}_1, \omega) \delta(\mathbf{k}_1 + \mathbf{k}_2). \tag{4.4}$$

Each diagram can be computed as nested integrals which typically look like

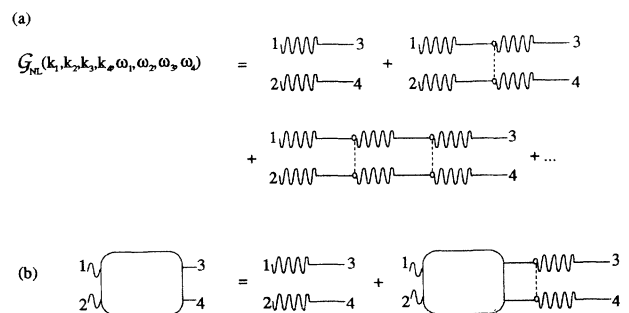


FIG. 4. Nonlinear Green's function.

$$\mathcal{H}(K) \int \frac{d\mathbf{k}_1 d\mathbf{k}_2 d\mathbf{k}_3 d\mathbf{k}_4 d\omega}{(2\pi)^9} \frac{d\omega}{2\pi} (\mathbf{k}_1 \cdot \mathbf{P}_k \cdot \mathbf{k}_2) [\delta(\mathbf{K}_3 + \mathbf{k}_1 + \mathbf{K}) - \delta(\mathbf{K}_3 + \mathbf{k}_1)] [\delta(\mathbf{K}_4 + \mathbf{k}_2 + \mathbf{K}) - \delta(\mathbf{K}_4 + \mathbf{k}_2)]$$

$$\times \mathcal{G}(\mathbf{k}_1, \mathbf{k}_3, \omega) \mathcal{G}(\mathbf{k}_2, \mathbf{k}_4, -\omega) \mathcal{H}(k) (\boldsymbol{\kappa}_1 \cdot \mathbf{P}_k \cdot \boldsymbol{\kappa}_2) [\delta(\mathbf{k}_3 + \boldsymbol{\kappa}_1 + \mathbf{k}) - \delta(\mathbf{k}_3 + \boldsymbol{\kappa}_1)] [\delta(\mathbf{k}_4 + \boldsymbol{\kappa}_2 + \mathbf{k}) - \delta(\mathbf{k}_4 + \boldsymbol{\kappa}_2)]. \quad (4.5)$$

The range of integration on the magnitude of the \mathbf{k} vectors is $[L^{-1}, \eta^{-1}]$. We will show that the integral contains a logarithmic divergence by considering the sub-range $k \in [L^{-1}, K]$. In this range the two-vector δ functions will not contribute, and we are left only with the Eulerian vertex. Implementing the δ functions the integral (4.5) becomes

$$\mathcal{H}(K) \int_{\mathbf{k}, \mathbf{k}_1, \mathbf{k}_2 \in [L^{-1}, K]} \frac{d\mathbf{k}_1 d\mathbf{k}_2 d\mathbf{k} d\omega}{(2\pi)^9} \frac{d\omega}{2\pi} (\mathbf{k}_1 \cdot \mathbf{P}_K \cdot \mathbf{k}_2)$$

$$\times \mathcal{G}(\mathbf{k}_1, \mathbf{k} + \boldsymbol{\kappa}_1, \omega) \mathcal{G}(\mathbf{k}_2, -\mathbf{k} + \boldsymbol{\kappa}_2, -\omega)$$

$$\times \mathcal{H}(k) (\boldsymbol{\kappa}_1 \cdot \mathbf{P}_k \cdot \boldsymbol{\kappa}_2) \dots \quad (4.6)$$

We can perform the integration over \mathbf{k}_1 and \mathbf{k}_2 using the form (4.4). The result, neglecting $\boldsymbol{\kappa}$ with respect to \mathbf{k} , reads

$$\mathcal{H}(K) \int_{\mathbf{k} \in [L^{-1}, K]} \frac{d\mathbf{k} d\omega}{(2\pi)^3} \frac{d\omega}{2\pi} (\mathbf{k} \cdot \mathbf{P}_K \cdot \mathbf{k})$$

$$\times |G(\mathbf{k}, \omega)|^2 \mathcal{H}(k) (\boldsymbol{\kappa}_1 \cdot \mathbf{P}_k \cdot \boldsymbol{\kappa}_2). \quad (4.7)$$

From the asymptotic properties of G at large frequencies we know that $|G(\mathbf{k}, \omega)|^2$ decays at least as fast as ω^{-2} . Thus the frequency integral converges. Using the scaling forms (2.20) and (3.7) and the result (3.29) we find that after integrating over the angles of \mathbf{k} the integral, denoted by I , is

$$I = \bar{\Delta} \int_{L^{-1}}^K \frac{dk}{k} = \bar{\Delta} \ln(LK). \quad (4.8)$$

The coefficient $\bar{\Delta}$ depends on the particular form and combination of the scaling functions. In a ladder diagram containing n rungs, only the first rung will not have this form. In order to have a divergence, we shall multiply also the first rung with $\mathbf{k}_1 \cdot \mathbf{k}_2$ and then we will get

$$\bar{\Delta}^n \int_{L^{-1}}^{\eta^{-1}} \frac{dk}{k} \int_{L^{-1}}^k \frac{dk_1}{k_1} \dots \int_{L^{-1}}^{k_{n-1}} \frac{dk_n}{k_n} = \frac{\bar{\Delta}^n}{n!} \ln^n(L/\eta). \quad (4.9)$$

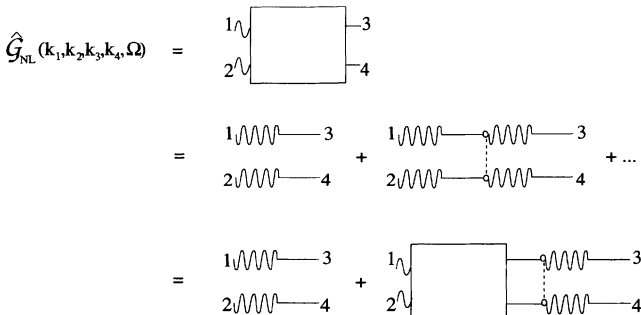


FIG. 5. Single-frequency nonlinear Green's function.

Obviously, when we resum such contributions the coefficient $\bar{\Delta}$ appears as an anomalous exponent:

$$\sum_{n=0}^{\infty} \frac{\bar{\Delta}^n}{n!} \ln^n \left(\frac{L}{\eta} \right) = \left(\frac{L}{\eta} \right)^{\bar{\Delta}}. \quad (4.10)$$

Another way to see the anomalous exponent is to return to the resummed equation Fig. 6 for the nonlinear Green's function. We will derive a resummed equation for a quantity $A(q, p, \Omega)$ defined by

$$\int \frac{d\mathbf{k}_1 d\mathbf{k}_2}{(2\pi)^6} \mathbf{k}_1 \cdot \mathbf{k}_2 \mathcal{G}_{NL}(\mathbf{k}_1, \mathbf{k}_2, \mathbf{q}, \mathbf{p}, \Omega)$$

$$= -\mathbf{q} \cdot \mathbf{p} G^{(2)}(q, p, \Omega) A(\mathbf{q}, \mathbf{p}, \Omega), \quad (4.11)$$

where

$$G^{(2)}(q, p, \Omega) = - \int \frac{d\omega}{(2\pi)} G(q, \omega) G(p, \Omega - \omega). \quad (4.12)$$

In this relation the coefficient of $A(q, p, \Omega)$ is the part that is the reproduced "tail" in the resummed diagrammatic series. $A(q, p, \Omega)$ can be understood as the contribution of the ladder. Notice that we have multiplied \mathcal{G}_{NL} explicitly by $\mathbf{k}_1 \cdot \mathbf{k}_2$ to achieve divergence. To derive an equation for $A(\mathbf{q}, \mathbf{p}, \Omega)$ we will substitute the resummed equation for $\mathcal{G}_{NL}(\mathbf{k}_1, \mathbf{k}_2, \mathbf{q}, \mathbf{p}, \Omega)$. The first term in $\mathcal{G}_{NL}(\mathbf{k}_1, \mathbf{k}_2, \mathbf{q}, \mathbf{p}, \Omega)$ gives

$$(2\pi) \int \frac{d\mathbf{k}_1 d\mathbf{k}_2 d\omega_1 d\omega_3}{(2\pi)^6} \frac{d\omega_1}{2\pi} \frac{d\omega_3}{2\pi}$$

$$\times \mathbf{k}_1 \cdot \mathbf{k}_2 \mathcal{G}(\mathbf{k}_1, \mathbf{p}, \omega_1) \mathcal{G}(\mathbf{k}_2, \mathbf{q}, \Omega - \omega_1) \delta(\omega_1 + \omega_3)$$

$$= -\mathbf{p} \cdot \mathbf{q} G^{(2)}(\mathbf{p}, \mathbf{q}, \Omega), \quad (4.13)$$

where we have again used the form (4.4). Referring to Fig. 5 the second term gives

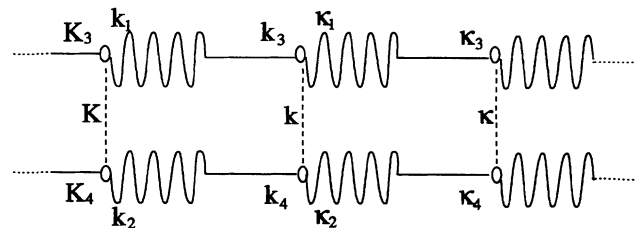


FIG. 6. Section of a diagram in the series for $\mathcal{G}_{NL}(\mathbf{k}_1, \mathbf{k}_2, \mathbf{k}_3, \mathbf{k}_4, \Omega)$.

$$\begin{aligned}
& \int \frac{d\mathbf{k}d\mathbf{p}'d\mathbf{q}'d\mathbf{p}''d\mathbf{q}''}{(2\pi)^9} \frac{d\omega}{2\pi} \mathbf{q}' \cdot \mathbf{p}' G^{(2)}(q', p', \Omega) A(\mathbf{q}', \mathbf{p}', \Omega) \\
& \quad \times \mathcal{H}(k)(\mathbf{q}'' \cdot \mathbf{P}_k \cdot \mathbf{p}'') \mathcal{G}(\mathbf{p}'', \mathbf{p}, \omega) \mathcal{G}(\mathbf{q}'', \mathbf{q}, \Omega - \omega) \delta(\mathbf{p}' + \mathbf{p}'' + \mathbf{k}) \delta(\mathbf{q}' + \mathbf{q}'' - \mathbf{k}) \\
& = - \int \frac{d\mathbf{k}}{(2\pi)^3} (\mathbf{p} + \mathbf{k}) \cdot (\mathbf{q} - \mathbf{k}) G^{(2)}(|\mathbf{q} - \mathbf{k}|, |\mathbf{p} + \mathbf{k}|, \Omega) A(\mathbf{q} - \mathbf{k}, \mathbf{p} + \mathbf{k}, \Omega) \mathcal{H}(k) (\mathbf{p} \cdot \mathbf{P}_k \cdot \mathbf{q}) G^{(2)}(q, p, \Omega).
\end{aligned} \tag{4.14}$$

To achieve a closed form equation for $A(\mathbf{q}, \mathbf{p}, \Omega)$ we consider the most divergent part in Eq. (4.11) which arises from the contribution proportional to k^2 in (4.14). This contribution comes from the region of integration $p, q \ll k$, which allows us to neglect \mathbf{p} and \mathbf{q} with respect to \mathbf{k} . Denoting $k^* \equiv \max[p, q]$ we combine now Eqs. (4.11)–(4.14) and cancel $\mathbf{p} \cdot \mathbf{q} G^{(2)}(\mathbf{p}, \mathbf{q}, \Omega)$ to arrive at

$$A(k^*, \Omega) = 1 + \frac{1}{3\pi^2} \int_{k^*} dk k^2 A(k, \Omega) G^{(2)}(k, k, \Omega) \mathcal{H}(k) k^2. \tag{4.15}$$

Here due to the limits on \mathbf{k} all the dependence on \mathbf{p} and \mathbf{q} has canceled, and remains only in the lower bound k^* in the integration, allowing us to replace the arguments of A by this value.

To proceed, we note that as a result of the scaling form for $G(k, \omega)$, $G^{(2)}(k, k, \Omega)$ must also be a function of Ω/k^z . For small Ω we can use the scaling relation (3.29) to arrive at the final equation

$$A(k^*) = 1 + \tilde{\Delta} \int_{k^*}^{\eta^{-1}} A(k) \frac{dk}{k}, \tag{4.16}$$

where $\tilde{\Delta}$ is determined as before by the coefficients of the various scaling functions. Taking the derivative of this equation with respect to k^* we find

$$\frac{dA(k^*)}{dk^*} = \tilde{\Delta} \frac{A(k^*)}{k^*}. \tag{4.17}$$

The solution of (4.17) is

$$A(k^*) = (\eta k^*)^{-\tilde{\Delta}}. \tag{4.18}$$

We refer to the exponent $\tilde{\Delta}$ as an “anomalous exponent.” Although we have used a form for the spatial dependence of the Green’s function (4.4) in demonstrating the existence of such a $\tilde{\Delta}$, the mechanism itself does not depend on this, although its numerical value will. We refer in future to the value of the anomalous exponent to be found using the true Green’s function as Δ . It is important to realize that, as in this case, it is possible to obtain an equation determining Δ , like Eq. (4.16), which is composed entirely of known quantities. The nonlinear Green’s function itself is composed of linear Green’s func-

tions, for which we have a closed form equation, Eq. (3.4). Therefore one may calculate explicitly the terms of the series for \mathcal{G}_{NL} and determine thereby their ratio. This is a task which we will leave to a future paper.

The aim of the rest of this paper is to show that the exponent Δ reappears in the evaluation of higher-order structure functions, as well as in the scaling exponent of the dissipation correlation functions.

V. HIGHER-ORDER CORRELATORS

A. The four-point simultaneous correlation function

The four-point correlation function of the quasi-Lagrangian passive field is defined by

$$\begin{aligned}
& 2\pi \mathcal{F}_4(\mathbf{k}_1, \mathbf{k}_2, \mathbf{k}_3, \mathbf{k}_4, \omega_1, \omega_2, \omega_3, \omega_4) \\
& \quad \times \delta(\omega_1 + \omega_2 + \omega_3 + \omega_4) \\
& = \langle \Theta(\mathbf{k}_1, \omega_1) \Theta(\mathbf{k}_2, \omega_2) \Theta(\mathbf{k}_3, \omega_3) \Theta(\mathbf{k}_4, \omega_4) \rangle.
\end{aligned} \tag{5.1}$$

We remind the reader that we have suppressed the r_0 label since we have chosen $r_0 = 0$. Integrating (5.1)

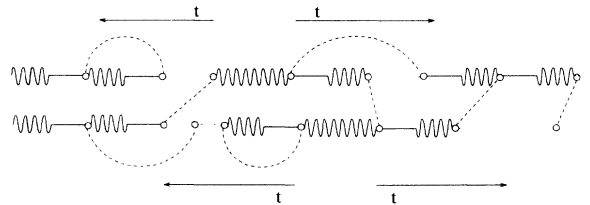


FIG. 7. Typical form of diagram in the series for $\hat{F}_4(\mathbf{k}_1, \mathbf{k}_2|\mathbf{k}_3, \mathbf{k}_4)$.

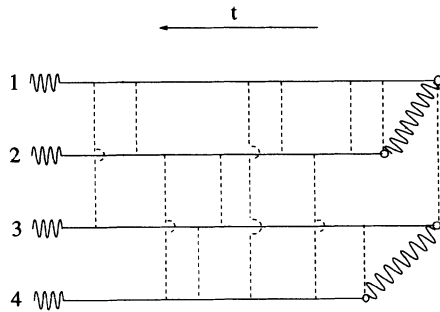


FIG. 8. Four-point correlator $\hat{F}_4(\mathbf{k}_1, \mathbf{k}_2, \mathbf{k}_3, \mathbf{k}_4)$ in time representation.

over all frequencies, we get the four-point simultaneous correlator $(2\pi)^3 F_4(\mathbf{k}_1, \mathbf{k}_2, \mathbf{k}_3, \mathbf{k}_4) \delta(\mathbf{k}_1 + \mathbf{k}_2 + \mathbf{k}_3 + \mathbf{k}_4)$. The diagrammatic expansion of the quantity is shown in Fig. 7. The structure of the diagram is based on two "highways" which consist of chains of Green's functions with only one correlator embedded, at which point the Green's functions change to complex conjugates. The two highways are connected both to themselves and to each other by the double velocity correlator dashed lines. Every highway connects two \mathbf{k} vectors, for example, \mathbf{k}_1 to \mathbf{k}_3 , and \mathbf{k}_2 to \mathbf{k}_4 . The whole set of diagrams is a sum of three contributions that we shall denote individually by $\hat{F}_4(\mathbf{k}_1, \mathbf{k}_2 | \mathbf{k}_3, \mathbf{k}_4)$, $\hat{F}_4(\mathbf{k}_1, \mathbf{k}_3 | \mathbf{k}_2, \mathbf{k}_4)$, and $\hat{F}_4(\mathbf{k}_1, \mathbf{k}_4 | \mathbf{k}_2, \mathbf{k}_3)$. Note that when the highway contains only the scalar correlation wavy line we obtain the Gaussian contribution to F_4 . Each \hat{F}_4 has one Gaussian contribution. We can thus focus now on one typical \hat{F}_4 and later take care of combinatorial factors.

To classify the diagrams for \hat{F}_4 it is useful to think about them in time representation. The time direction is shown by the arrows in Fig. 7. To take advantage of this time ordering, we shall redraw the diagrams as shown in Fig. 8. In this representation points on a vertical axis share the same time. It is now obvious that the double velocity correlators should all be vertical in the limit $(\gamma/\Gamma) \rightarrow 0$. Only connections with vertical dashed lines between the highways are not suppressed by the factor $(\gamma/\Gamma) \rightarrow 0$. Notice that the wavy line of the scalar correlator is allowed to have any slope.

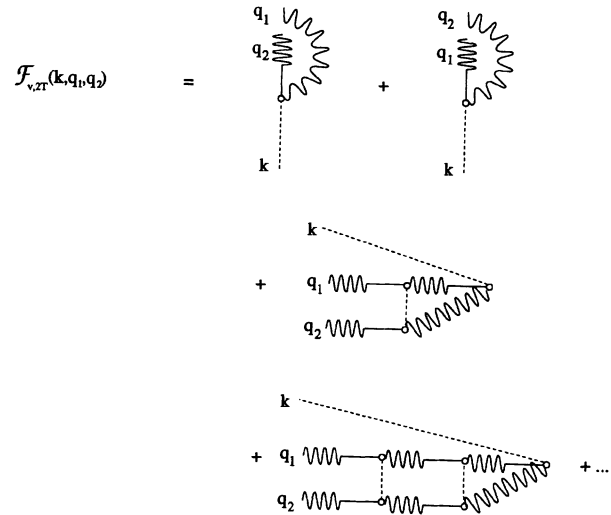


FIG. 9. Three-point correlator $F_{v,2T}$.

B. Simultaneous higher-order correlations of \mathbf{v} and Θ

We begin by computing the correlation

$$\mathbf{F}_{v,2T}(\mathbf{k}, \mathbf{q}_1, \mathbf{q}_2) (2\pi)^3 \delta(\mathbf{k} + \mathbf{q}_1 + \mathbf{q}_2) = \langle \mathbf{v}(\mathbf{k}, t) T(\mathbf{q}_1, t) T(\mathbf{q}_2, t) \rangle. \quad (5.2)$$

Using the expansion for $\Theta(\mathbf{k}_1, t)$ we find the diagrammatic series for $\langle \mathbf{v}(\mathbf{k}, t) \Theta(\mathbf{q}_1, t) \Theta(\mathbf{q}_2, t) \rangle$, the first few terms of which are shown in Fig. 9, in time representation. This correlation function is identical to the desired correlation (5.2) because for a same-time quantity the Eulerian and quasi-Lagrangian quantities coincide. Also, we do not need to carry the time explicitly, since the quantity is time independent. The first two diagrams are the only surviving ones in the limit $(\gamma/\Gamma) \rightarrow 0$. This is because all higher-order diagrams must contain a nonvertical velocity correlation dashed line. Those higher order diagrams in which the extra dashed line of the $\mathcal{H}(\mathbf{k})$ is vertical must have that line at the first vertex, as in the first two terms. Such diagrams are already included in the resummation into the first diagram. The first two diagrams read

$$\langle \mathbf{v}(\mathbf{k}) T(\mathbf{q}_1) T(\mathbf{q}_2) \rangle = \int \frac{d\mathbf{k}_1 d\mathbf{k}_2 d\omega_1 d\omega_2}{(2\pi)^8} \mathcal{H}(\mathbf{k}) \cdot [\mathcal{V}(\mathbf{k}_1, \mathbf{k}, \mathbf{k}_2) \mathcal{G}(\mathbf{q}_1, \mathbf{k}_1, \omega_1) \mathcal{F}(\mathbf{q}_2, \mathbf{k}_2, \omega_2) + \mathcal{V}(\mathbf{k}_2, \mathbf{k}, \mathbf{k}_1) \mathcal{G}(\mathbf{q}_2, \mathbf{k}_2, \omega_2) \mathcal{F}(\mathbf{q}_1, \mathbf{k}_1, \omega_1)]. \quad (5.3)$$

This gives

$$\mathbf{F}_{v,2T}(\mathbf{k}, \mathbf{q}_1, \mathbf{q}_2) = -\frac{i}{2} \mathcal{H}(k) \mathbf{P}_k \cdot [\mathbf{q}_2 F(q_2) + \mathbf{q}_1 F(q_1)]. \quad (5.4)$$

Notice that the non-Eulerian contributions in the vertex cancel exactly.

It is also straightforward to compute the simultaneous correlation $\mathbf{F}_{v,4T}(\mathbf{k}, \mathbf{q}_1, \mathbf{q}_2, \mathbf{q}_3, \mathbf{q}_4)$ which is defined analogously to (5.2). Since we have displayed already the

diagram for F_4 , it is easy to see that the diagram for this new quantity is the one shown in Fig. 10. To see that this is the only possible configuration remember that to average our scalar quantity F_4 against a $\mathbf{v}(\mathbf{k}, t)$ we need to expose a vertex that contains another factor of $\mathbf{v}(\mathbf{k}, t)$. This results in an additional Green's function and a two-point velocity correlator. As all the exposed legs must have the same time label, and the dashed line must be vertical, it is obvious that Fig. 10 together with the permutations of the exposed legs is the quantity that we are seeking. Analytically we have

$$\begin{aligned} & \langle \mathbf{v}(\mathbf{k})T(\mathbf{q}_1)T(\mathbf{q}_2)T(\mathbf{q}_3)T(\mathbf{q}_4) \rangle \\ &= \int \frac{d\mathbf{p}d\mathbf{p}'}{(2\pi)^6} \frac{d\omega}{2\pi} \mathcal{G}(\mathbf{q}_1, \mathbf{p}', \omega) \mathcal{V}(\mathbf{p}', \mathbf{k}, \mathbf{p}) \mathcal{H}(\mathbf{k}) \\ & \quad \times F_4(\mathbf{p}, \mathbf{q}_2, \mathbf{q}_3, \mathbf{q}_4) \delta(\mathbf{p} + \mathbf{q}_2 + \mathbf{q}_3 + \mathbf{q}_4) \\ & \quad + (\text{three other permutations}). \end{aligned} \quad (5.5)$$

Integrating the Green's function over frequencies gives a δ function $(2\pi)^3 \delta(\mathbf{p}' + \mathbf{q}_1)$, so we may perform immediately the integration over \mathbf{p}' to obtain for the first of the four contributions

$$\begin{aligned} \mathbf{F}_{v,4T}(\mathbf{k}, \mathbf{q}_1, \mathbf{q}_2, \mathbf{q}_3, \mathbf{q}_4) &= -\frac{i}{2} \mathcal{H}(\mathbf{k}) \mathbf{P}_k \cdot \left[\mathbf{q}_1 F_4(\mathbf{q}_1 + \mathbf{k}, \mathbf{q}_2, \mathbf{q}_3, \mathbf{q}_4) + \mathbf{q}_2 F_4(\mathbf{q}_1, \mathbf{q}_2 + \mathbf{k}, \mathbf{q}_3, \mathbf{q}_4) \right. \\ & \quad \left. + \mathbf{q}_3 F_4(\mathbf{q}_1, \mathbf{q}_2, \mathbf{q}_3 + \mathbf{k}, \mathbf{q}_4) + \mathbf{q}_4 F_4(\mathbf{q}_1, \mathbf{q}_2, \mathbf{q}_3, \mathbf{q}_4 + \mathbf{k}) \right]. \end{aligned} \quad (5.7)$$

Comparing (5.4) and (5.7) one can see how the equation for $\mathbf{F}_{v,2nT}$ appears:

$$\begin{aligned} \mathbf{F}_{v,2nT}(\mathbf{k}, \mathbf{q}_1, \dots, \mathbf{q}_{2n}) &= -\frac{i}{2} \mathcal{H}(k) \cdot [\mathbf{q}_1 F_{2n}(\mathbf{q}_1 + \mathbf{k}, \mathbf{q}_2, \dots, \mathbf{q}_{2n}) + \mathbf{q}_2 F_{2n}(\mathbf{q}_1, \mathbf{q}_2 + \mathbf{k}, \dots, \mathbf{q}_{2n}) \\ & \quad + \dots + \mathbf{q}_{2n} F_{2n}(\mathbf{q}_1, \mathbf{q}_2, \dots, \mathbf{q}_{2n} + \mathbf{k})]. \end{aligned} \quad (5.8)$$

C. Structure functions

In this section we consider the functions $S_{2n}(r)$, $\mathcal{D}_{2n}(r)$, and $J_{2n}(r)$, defined in Eqs. (1.1), (1.10), and (1.11). The n -order structure function of the scalar field is related to F_{2n} by

$$\begin{aligned} S_{2n}(r) &= (2\pi)^3 \int \prod_{j=1}^{2n} \frac{d\mathbf{k}_j}{(2\pi)^3} [1 - \exp(i\mathbf{k}_j \cdot \mathbf{r})] \\ & \quad \times \delta \left(\sum_{m=1}^{2n} \mathbf{k}_m \right) F_{2n}(\mathbf{k}_1, \dots, \mathbf{k}_{2n}). \end{aligned} \quad (5.9)$$

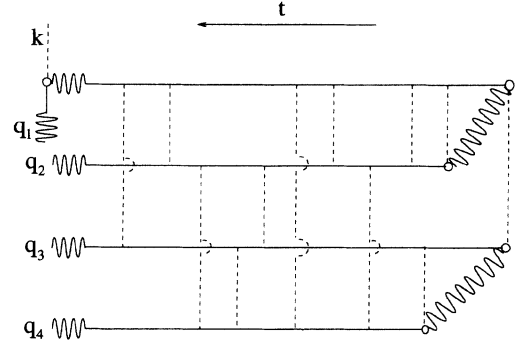


FIG. 10. $F_{v,4T}$ in time representation: schematic of a typical term.

$$\begin{aligned} & -\frac{i}{2} \mathcal{H}(\mathbf{k}) \int d\mathbf{p} \mathbf{p} \cdot \mathbf{P}_k F_4(\mathbf{p}, \mathbf{q}_2, \mathbf{q}_3, \mathbf{q}_4) \delta(\mathbf{p} + \mathbf{q}_2 + \mathbf{q}_3 + \mathbf{q}_4) \\ & \quad \times [\delta(\mathbf{q}_1 + \mathbf{k} + \mathbf{p}) - \delta(\mathbf{q}_1 + \mathbf{p})]. \end{aligned} \quad (5.6)$$

When we perform the integration over \mathbf{p} we again find that the contributions from the non-Eulerian δ functions cancel. As in the case of the three-point correlator $\langle \mathbf{v}TT \rangle$, only the Eulerian vertex contributes to the final result,

Similarly we can define $J_{2n}(r)$ in terms of F_{2n} :

$$\begin{aligned} J_{2n}(r) &= -2n(2\pi)^3 \kappa \int k_1^2 \prod_{j=1}^{2n} \frac{d\mathbf{k}_j}{(2\pi)^3} [1 - \exp(i\mathbf{k}_j \cdot \mathbf{r})] \\ & \quad \times \delta \left(\sum_{m=1}^{2n} \mathbf{k}_m \right) F_{2n}(\mathbf{k}_1, \dots, \mathbf{k}_{2n}). \end{aligned} \quad (5.10)$$

Finally, \mathcal{D}_{2n} is written as

$$\mathcal{D}_{2n}(r) = in(2\pi)^3 \int \frac{d\mathbf{k}}{(2\pi)^3} \prod_{j=1}^{2n} \frac{d\mathbf{q}_j}{(2\pi)^3} \{1 - \exp[i(\mathbf{k}\delta_{j,2n} + \mathbf{q}_j) \cdot \mathbf{r}]\} \delta\left(\mathbf{k} + \sum_{m=1}^{2n} \mathbf{q}_m\right) \mathbf{q}_{2n} \cdot \mathbf{F}_{v,2nT}(\mathbf{k}, \mathbf{q}_1, \dots, \mathbf{q}_{2n}). \tag{5.11}$$

To analyze $\mathcal{D}_{2n}(r)$, we substitute for $\mathbf{F}_{v,2nT}$ Eq. (5.8); rearranging, and using the δ functions and the symmetry of F_{2n} with respect to all its arguments, we obtain

$$\begin{aligned} \mathcal{D}_{2n}(r) = n(2n-1)(2\pi)^3 \int \frac{d\mathbf{k}d\mathbf{q}_1d\mathbf{q}_2}{(2\pi)^9} \prod_{j=3}^{2n} \frac{d\mathbf{q}_j}{(2\pi)^3} [1 - \exp(i\mathbf{q}_j \cdot \mathbf{r})] \{1 - \exp[i(\mathbf{k} + \mathbf{q}_1) \cdot \mathbf{r}]\} [1 - \exp(i\mathbf{q}_2 \cdot \mathbf{r})] \\ \times [\mathbf{q}_1 \cdot \mathcal{H}(\mathbf{k}) \cdot \mathbf{q}_2] \delta\left(\mathbf{k} + \sum_{m=1}^{2n} \mathbf{q}_m\right) [F_{2n}(\mathbf{q}_1, \mathbf{q}_2 + \mathbf{k}, \dots, \mathbf{q}_{2n}) - F_{2n}(\mathbf{q}_1 + \mathbf{k}, \mathbf{q}_2, \dots, \mathbf{q}_{2n})]. \end{aligned} \tag{5.12}$$

From this form it will be very useful to proceed to determine a differential relation between $\mathcal{D}_{2n}(r)$ and $S_{2n}(r)$. It is convenient to make use of an identity

$$\begin{aligned} \text{Re} \left\{ \prod_{j=1}^{2n} [1 - \exp(i\mathbf{q}_j \cdot \mathbf{r})] \right\} \delta(\mathbf{q}_1 + \mathbf{q}_2 + \dots + \mathbf{q}_{2n}) \\ = 2\text{Re} \left\{ \prod_{j=2}^{2n} [1 - \exp(i\mathbf{q}_j \cdot \mathbf{r})] \right\} \delta(\mathbf{q}_1 + \mathbf{q}_2 + \dots + \mathbf{q}_{2n}). \end{aligned} \tag{5.13}$$

Then one may immediately replace in the above expression the factor $1 - \exp[i(\mathbf{k} + \mathbf{q}_1) \cdot \mathbf{r}]$ by 2. Let us focus now only on the factors

$$\begin{aligned} [1 - \exp(i\mathbf{q}_2 \cdot \mathbf{r})] \delta\left(\mathbf{k} + \sum_{m=1}^{2n} \mathbf{q}_m\right) \\ \times [F_{2n}(\mathbf{q}_1, \mathbf{q}_2 + \mathbf{k}, \dots, \mathbf{q}_{2n}) - F_{2n}(\mathbf{q}_1 + \mathbf{k}, \mathbf{q}_2, \dots, \mathbf{q}_{2n})]. \end{aligned} \tag{5.14}$$

In the first term let us make the transformation $\mathbf{q}_2 + \mathbf{k} \rightarrow \mathbf{q}_2$ and in the second $\mathbf{q}_1 + \mathbf{k} \rightarrow \mathbf{q}_1$. Such a substitution will not affect the remaining terms of the expression for \mathcal{D}_{2n} due to the orthogonality of $\mathcal{H}(\mathbf{k})$ and \mathbf{k} . Elementary manipulations show that (5.14) now becomes

$$\begin{aligned} \exp(i\mathbf{q}_2 \cdot \mathbf{r}) [1 - \exp(-i\mathbf{k} \cdot \mathbf{r})] \delta\left(\sum_{m=1}^{2n} \mathbf{q}_m\right) \\ \times F_{2n}(\mathbf{q}_1, \mathbf{q}_2, \dots, \mathbf{q}_{2n}). \end{aligned} \tag{5.15}$$

Now substituting back into the full expression for \mathcal{D}_{2n} and defining the tensor of velocity differences in r space

$$\mathbf{h}(\mathbf{r}) \equiv \int \frac{d\mathbf{k}}{(2\pi)^3} [1 - \exp(-i\mathbf{k} \cdot \mathbf{r})] \mathcal{H}(\mathbf{k}), \tag{5.16}$$

we find that \mathcal{D}_{2n} takes the form

$$\begin{aligned} \mathcal{D}_{2n}(r) = h_{\alpha\beta}(\mathbf{r})(2\pi)^3 \int \frac{d\mathbf{q}_1}{(2\pi)^3} \frac{d\mathbf{q}_2}{(2\pi)^3} \prod_{j=3}^{2n} \frac{d\mathbf{q}_j}{(2\pi)^3} [1 - \exp(i\mathbf{q}_j \cdot \mathbf{r})] \\ \times q_{1\alpha} q_{2\beta} \exp(i\mathbf{q}_2 \cdot \mathbf{r}) \delta\left(\sum_{m=1}^{2n} \mathbf{q}_m\right) F_{2n}(\mathbf{q}_1, \mathbf{q}_2, \dots, \mathbf{q}_{2n}). \end{aligned} \tag{5.17}$$

The function \mathbf{h} as defined in Eq. (5.16) has the same scaling as the eddy diffusivity, Eq. (1.13), i.e., $\mathbf{h}(\mathbf{r}) \sim r^{\zeta_h}$. Now examining the expression for $S_{2n}(r)$, it is easy to show that

$$\begin{aligned} \nabla_\alpha \nabla_\beta S_{2n}(r) &= 2n(2n-1)(2\pi)^3 \int \frac{d\mathbf{q}_1 d\mathbf{q}_2}{(2\pi)^6} \prod_{j=3}^{2n} \frac{d\mathbf{q}_j}{(2\pi)^3} [1 - \exp(i\mathbf{q}_j \cdot \mathbf{r})] \\ &\times q_{1\alpha} q_{2\beta} \exp(i\mathbf{q}_2 \cdot \mathbf{r}) \delta \left(\sum_{m=1}^{2n} \mathbf{q}_m \right) F_{2n}(\mathbf{q}_1, \mathbf{q}_2, \dots, \mathbf{q}_{2n}), \end{aligned} \tag{5.18}$$

which shows directly that

$$\mathcal{D}_{2n}(r) = h_{\alpha\beta}(r) \nabla_\alpha \nabla_\beta S_{2n}(r). \tag{5.19}$$

Projecting this into scalar form and using the divergence-free nature of $\mathbf{h}(r)$ one obtains the differential equation given by Eq. (1.12).

For future reference it is useful to write J_{2n} in terms of reducible and irreducible contributions with respect to a pair of k_i variables in F_{2n} . Therefore we decompose $F_{2n}(\mathbf{q}_1, \dots, \mathbf{q}_{2n})$ into a sum of reducible and irreducible parts with respect to the first two arguments, where the latter is denoted with a tilde:

$$\begin{aligned} F_{2n}(\mathbf{q}_1, \dots, \mathbf{q}_{2n}) &= (2\pi)^3 F_2(\mathbf{q}_1) \delta(\mathbf{q}_1 + \mathbf{q}_2) F_{2n-2}(\mathbf{q}_3, \dots, \mathbf{q}_{2n}) \\ &\quad + \tilde{F}_{2n}(\mathbf{q}_1, \mathbf{q}_2 | \mathbf{q}_3, \dots, \mathbf{q}_{2n}). \end{aligned} \tag{5.20}$$

Then we can write J_{2n} in terms of reducible and irreducible contributions in the same sense. In the integral \mathbf{k}_1 is special and will be one of the \mathbf{k} vectors in the pair. The other one can be any of the vectors $\mathbf{k}_2, \dots, \mathbf{k}_{2n}$:

$$J_{2n}(r) = n(2n-1)J_2(r)S_{2n-2}(r) + \tilde{J}_{2n}(r), \tag{5.21}$$

where \tilde{J}_{2n} is given in terms of \tilde{F}_{2n} as J_{2n} is given in terms of F_{2n} . Using the same decomposition (5.20) in (1.1) we get

$$S_{2n}(r) = n(2n-1)S_2(r)S_{2n-2}(r) + \tilde{S}_{2n}(r). \tag{5.22}$$

In the following section we will make use of this decomposition to compare the contributions due to normal scaling and that of the anomalous terms.

VI. THE ANOMALOUS EXPONENT IN THE STRUCTURE FUNCTIONS

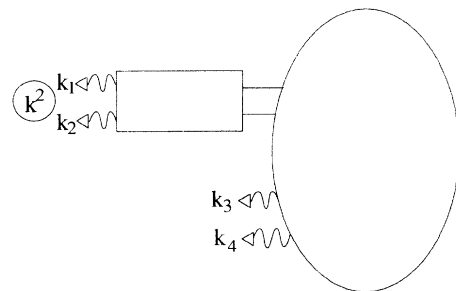
In this section we collect the results of the preceding sections with the aim of understanding the origin of the anomalous scaling of the structure functions. The situation can be clarified completely within the analysis of J_4 and S_4 .

The calculation of J_4 and S_4 is based on the diagrams for F_4 , which are shown in Fig. 8. The diagrams for F_4 have the structure discussed in the preceding section, within which series is contained a sequence which has the form of a ladder as introduced in terms of the nonlinear Green's function in Sec. IV, here multiplied also by some other terms. The difference between the calculation of

J_4 and S_4 lies only in the addition of a factor of k_1^2 in the case of J_4 . Without this factor of k^2 , every diagram in the series of J_4 converges in both the ir and the uv. After the addition of the k^2 factor each diagram will gain a logarithmic divergence via the same mechanism that we discussed in detail in Sec. IV. These diverging logarithms can be as before resummed into the ladder contribution, giving an important contribution to \tilde{J}_4 that we represent in Fig. 11. This contribution is obtained from the range of integration in which the two \mathbf{k} vectors \mathbf{k}_1 and \mathbf{k}_2 are large.

We need to argue that the exponent Δ which appears here is the same Δ which appeared previously, and whose value we can calculate as outlined in Sec. IV. The reason for this is that the ladder series have the same topology. The terms which arise in J_4 differ slightly from those in the calculation of A [defined in Eq. (4.11)] in the prefactor $[1 - \exp(i\mathbf{k}_1 \cdot \mathbf{r})][1 - \exp(i\mathbf{k}_2 \cdot \mathbf{r})]$, and in the appearance of k_1^2 instead of $\mathbf{k}_1 \cdot \mathbf{k}_2$. Let us return to the argument given in Sec. IV concerning the nonlinear Green's function, where we obtained a multiplicative series of nested integrals displayed in Eq. (4.8). These differences will affect only the first multiple, after which each term will contribute a factor of Δ in the coefficient, and for the infinite series the value of the exponent will not be affected. In any case, for large $\mathbf{k}_1, \mathbf{k}_2$, the exponential term is negligible, and the difference between a prefactor of $\mathbf{k}_1 \cdot \mathbf{k}_2$ and k_1^2 is only an integration by parts. Therefore it is clear that the value of Δ arises out of the structure of the repeating terms in the ladder and will not be affected by the details of the initial terms.

To continue, we see that the resummed sequence in J_4 will contribute a large factor of the order of $(r/\eta)^\Delta$ compared with the remaining contributions that we do not consider explicitly. The details of the remainder of the diagram are not important and are represented in Fig. 11



$$k \triangleleft = 1 - \exp(ik \cdot r)$$

FIG. 11. Schematic representation of $J_4(r)$.

by the “egg.” In addition to this important contribution to $J_4(r)$, there is the contribution that arises from the reducible part which equals $6J_2S_2$; see Eq. (5.21). Using the differential equation Eq. (1.12) and the balance equation (1.9) for the case $n = 1$, one obtains

$$J_2 = 6\kappa\zeta_2(T)h(r)\frac{S_2(r)}{r^2} = 6\kappa\zeta_2(T)Fh(0), \quad (6.1)$$

where we have made use of the scaling relation (3.31). Adding the two major contributions we can write

$$J_4(r) \simeq 6 \left[\kappa C_4 \left(\frac{r}{\eta} \right)^\Delta \frac{\tilde{S}_4(r)}{r^2} + J_2 S_2(r) \right]. \quad (6.2)$$

In achieving Eq. (6.2) we need to convince ourselves that contributions to the diagram in which three or four \mathbf{k} vectors are large, i.e., of the order of $1/\eta$, are negligible compared with the displayed contribution with two large \mathbf{k} vectors. Consider first the case with four large \mathbf{k} vectors. Since the separation distance appears only in the exponential factors, and their contribution disappears for large \mathbf{k} , the resulting diagram is independent of the separation distance. In this case, by dimensional reasoning, all the diagrams should be of the same order for $r \simeq \eta$. Therefore we may evaluate their contribution from the above estimation (6.2) at $r = \eta$. Accordingly the contribution with four large \mathbf{k} 's is small. The case when three \mathbf{k} 's are large is also negligible. Consider first the small \mathbf{k} leg which connects to the egg, where all other incoming \mathbf{k} vectors are large, through a Green's function. The local integral at this entry point is of the order of $\int d\mathbf{k}d\omega \mathbf{k}G(\mathbf{k}, \omega)$, where the \mathbf{k} is the estimate of the vertex. After integrating over frequencies, this integral is of the order of $\int d\mathbf{k} \mathbf{k}$, which contributes in the uv. This has been taken into account in the four large \mathbf{k} vector contribution. If the incoming leg has a correlator instead of a Green's function, we use the symmetry of the correlator under $\mathbf{k} \rightarrow -\mathbf{k}$ to see that the first-order contribution in k vanishes, and the next order again contributes mostly in the uv.

Equation (6.2) can be used now in conjunction with Eqs. (1.9) and (5.22) to write the balance equation

$$\begin{aligned} & 6 \left[\kappa C_4 \left(\frac{r}{\eta} \right)^\Delta \frac{\tilde{S}_4(r)}{r^2} + J_2 S_2(r) \right] \\ & = K_1(\zeta_2(T))J_2S_2 + K_2(\tilde{\zeta}_4, \zeta_h) \frac{h(r)\tilde{S}_4(r)}{r^2}, \quad (6.3) \end{aligned}$$

where $\tilde{\zeta}_{2n}$ has the obvious meaning of the scaling exponent of \tilde{S}_{2n} . The coefficients $K_1 = 8\zeta_2^2$ and $K_2 = 4\tilde{\zeta}_4(4\tilde{\zeta}_4 + \zeta_h + 1)$ are determined by the differential equation (1.12). The question as to whether there is or is not anomalous scaling in S_4 now depends crucially on the numerical value of the anomalous exponent Δ . If, on the LHS, the term in Δ is negligible in comparison to the simple scaling term, then on the RHS one must have $\tilde{\zeta}_4 = \zeta_2$. This implies a critical value of Δ as the point where the scaling of the term in Δ balances the simple scaling term, i.e., $\Delta_{\text{crit}} = \zeta_h$. Therefore we predict that

for $\Delta < \Delta_{\text{crit}}$, $\tilde{S}_4(r) \propto S_2^2(r)$ in the limit $\kappa \rightarrow 0$. We stress that this does not mean that there may not be serious corrections to scaling as Δ approaches ζ_h . When Δ reaches the critical value ζ_h , $\tilde{S}_4(r)$ gains anomalous scaling and becomes the dominant term. Further analysis of this situation in the context of the Navier-Stokes dynamics has been presented in [25]. Our present control of the theory, and in particular of the coefficients of the scaling functions, does not allow us to compute all coefficients completely. This is where we cannot repeat the analysis that was sketched after Eq. (1.13) in the Introduction. Regrettably, we think that the difference between our findings and the assumptions of Kraichnan will not go away. We have exhausted already the benefit that could be extracted from the separation of time scales between the velocity field and the scalar field, and we believe therefore that some of the assumptions used by Kraichnan are uncontrolled. Therefore we believe that Eq. (1.15) which relates the values of ζ_{2n} to ζ_2 is incorrect.

We have previously seen that Δ may be computed from first principles through the nonlinear Green's function. We show now that it is also an experimentally measurable quantity. To this end we turn to the analysis of the two-point correlation function of the dissipation fluctuations. We find that Δ appears measurably in this correlation function. We will show in the following section that the critical value Δ_{crit} reappears in this context.

VII. THE DISSIPATION CORRELATION FUNCTION

The aim of this section is to calculate the scaling exponent of the two-point correlation function $K(r)$ of the dissipation field $\epsilon(\mathbf{x}, t) \equiv \kappa|\nabla T(\mathbf{x}, t)|^2$, which plays in our problem the same role as the energy dissipation rate in Navier-Stokes dynamics:

$$K(r) = \langle \epsilon(\mathbf{x} + \mathbf{r}, t)\epsilon(\mathbf{x}, t) \rangle - \langle \epsilon(\mathbf{x}, t) \rangle^2. \quad (7.1)$$

We will argue that the decay properties of $K(r)$ with r are strongly influenced by the presence or otherwise of multiscaling. In a separate paper [25], we shall show that in cases in which $K(r)$ decays slowly with r we will expect corrections to scaling, but not true multiscaling.

We first evaluate the Gaussian contribution to $K(r)$, denoted as $K_G(r)$. Rewrite (7.1) as

$$\begin{aligned} K(r) & = \langle \nabla_\alpha T(\mathbf{x} + \mathbf{r}) \nabla_\alpha T(\mathbf{x} + \mathbf{r}) \\ & \quad \times \nabla_\beta T(\mathbf{x}) \nabla_\beta T(\mathbf{x}) \rangle - \langle \epsilon \rangle^2. \quad (7.2) \end{aligned}$$

There are three Gaussian contributions, one of which cancels $\langle \epsilon \rangle^2$, and we are left with

$$K_G(r) = 2 \langle \nabla_\alpha T(\mathbf{x} + \mathbf{r}) \nabla_\beta T(\mathbf{x}) \rangle \langle \nabla_\alpha T(\mathbf{x} + \mathbf{r}) \nabla_\beta T(\mathbf{x}) \rangle. \quad (7.3)$$

In order to determine the scaling exponents of the contribution we relate it to $S_2(r)$. It is easy to see that $K_g(r)$ and $S_2(r)$ are related by the exact expression

$$K_g(r) = \frac{1}{2} \frac{\partial^2 S_2(r)}{\partial r_\alpha \partial r_\beta} \frac{\partial^2 S_2(r)}{\partial r_\alpha \partial r_\beta} \propto r^{4[\zeta_2(T)-1]}. \quad (7.4)$$

Note that this exponent is negative.

To calculate the total scaling behavior of $K(r)$, we need now to also consider the irreducible contribution $K^{(irr)}(r)$, which can be related to F_4 according to

$$\begin{aligned} K^{(irr)}(r) &= (2\pi)^3 \int \prod_{j=1}^4 \frac{d\mathbf{k}_j}{2\pi} \exp[i(\mathbf{k}_1 + \mathbf{k}_2) \cdot \mathbf{r}] \\ &\times (\mathbf{k}_1 \cdot \mathbf{k}_2)(\mathbf{k}_3 \cdot \mathbf{k}_4) \delta\left(\sum_{m=1}^4 \mathbf{k}_m\right) \\ &\times F_4^{(irr)}(\mathbf{k}_1, \dots, \mathbf{k}_4), \end{aligned} \quad (7.5)$$

where $F_4^{(irr)}$ is the irreducible part of F_4 . As in the quantities that we discussed in Secs. IV and VI, the largest contribution to (7.5) comes from the regime of large \mathbf{k} vectors. In fact, the regime $\mathbf{k}_1, \mathbf{k}_2, \mathbf{k}_3$, and $\mathbf{k}_4 \sim 1/\eta \gg 1/r$ is the most important one. However the exponent forces upon us the additional constraints $|\mathbf{k}_1 + \mathbf{k}_2| \sim 1/r$, and due to the δ function also $|\mathbf{k}_3 + \mathbf{k}_4| \sim 1/r$. The regime in which all the \mathbf{k} vectors are of the order of $1/r$ (the local contributions) leads to a scaling behavior that is identical to the Gaussian contribution, as simple power counting in (7.5) will show. We are thus led to consider the diagram in Fig. 12. It has now two ladder contributions, connected by an "egg." Since $|\mathbf{k}_1 + \mathbf{k}_2| \sim 1/r$, and the same for $|\mathbf{k}_3 + \mathbf{k}_4|$, the \mathbf{k} vector κ that connects the two ladders is of the order of $1/r$ or smaller. We can estimate the contribution from the ladders to the diagrams as $(r/\eta)^{2\Delta}$. The quantity $K^{(irr)}(r)$ is of the order of $K_G(r)(r/\eta)^{2\Delta}$. Writing the Gaussian and the irreducible contributions together we get finally

$$\begin{aligned} K(r) &= K_G(r) [1 + C(r/\eta)^{2\Delta}] \\ &\simeq r^{4[\zeta_2(T)-1]} + \tilde{C} r^{4[\zeta_2(T)-1]+2\Delta}. \end{aligned} \quad (7.6)$$

It is important to realize here that due to the negative sign of the exponents, the anomalous contribution will dominate for all nonzero Δ , allowing Δ to be experimentally observable even in subcritical conditions.

Note that a similar result for the correlation of the energy dissipation rate in "usual" hydrodynamics was found in Ref. [19]. Using the condition for multiscal-

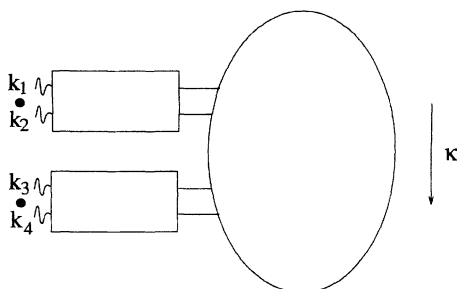


FIG. 12. Representation of $K(r)$.

ing (6.3) and the scaling relation (3.31) we discover that normal scaling is destroyed when

$$K(r) \sim r^0. \quad (7.7)$$

If Δ is too small to destroy normal scaling in the structure functions, it is also too small to compensate the decay of $K(r)$ that is caused by the Gaussian contributions. *Mutatis mutandis*, when Δ is large enough to lead to a high correlation between dissipative events which are separated by r in the "inertial range," then the very notion of the "inertial range" becomes untenable. These dissipative effects show up throughout the scaling range via an anomalous contribution in the structure functions.

VIII. SUMMARY AND DISCUSSION

The main result of this paper is the demonstration of a mechanism for the destruction of normal scaling in this model of a passive scalar driven by a fast-varying velocity field. This mechanism stems from the accumulation of the effects of the dissipative processes that cannot be eliminated even when the scale of interest is much larger than the traditionally defined dissipative scale. This anomalous exponent appears very cleanly in the nonlinear Green's function and in the two-point correlation function of the dissipation $K(r)$. From the point of view of the latter quantity the central result of this paper is Eq. (7.6). The very same anomalous exponent reappears in the structure functions of the scalar field as a term competing with the Gaussian term which by itself would lead to simple scaling. We found that when the correlation function $K(r)$ stops decaying for r even in the scaling range, the anomalous term in the structure functions becomes dominant.

It is interesting to notice that in this problem we have some external control on the appearance of anomalous scaling. Let us return to the rigorous bound (1.6). Assume that there is no anomalous scaling, and then $\zeta_2 = \zeta_\infty$. The bound then implies that

$$2\zeta_2 + \zeta(u) \leq 1, \quad \text{condition for normal scaling.} \quad (8.1)$$

Writing as in Eq. (2.20) $\mathcal{H}(k)$ but now with the additional exponents

$$H(k) \sim k^{y(u)} \text{ and } \Gamma_k \sim k^{z(u)}, \quad (8.2)$$

we can easily use the scaling relations (3.29) and (3.31) to conclude that (8.1) is only obeyed if

$$z(u) \leq \zeta(u) - 1. \quad (8.3)$$

Obviously, as long as (8.3) is obeyed, we can have normal scaling in (6.3), implying that $\Delta < \zeta_h$. When (8.3) is violated, we must lose normal scaling. Since the violation of (8.3) can be achieved by choosing appropriately the parameters of the driving velocity field, this model must allow multiscaling. It would be interesting to determine whether the violation of (8.3) and the crossing of Δ_{crit} by Δ occur in a related fashion.

Note that our theoretical development is somewhat

dangerous. In all our work we have neglected the term κk^2 in the bare Green's function, arguing that for k in the inertial range this term is small. On the other hand, multiplying by k^2 various diagrams in the theory resulted in divergences that led to anomalous scaling. It may be checked that expanding the Green's function to expose the κk^2 contributions results in a ladder sequence that is of higher order in γ/Γ . The appearance of κ in S_{2n} occurs in our theory in a nonperturbative way through the balance equation, which is not an order-by-order relation.

A separate issue is that in evaluating the diagrams with ladders and "eggs" as the ladder contribution times simple scaling contributions is really justified only as long as $\Delta \leq \zeta_h$. When Δ exceeds ζ_h the "eggs" may contain other divergent contributions that we have no control over. Therefore our theory should be considered as rigorous only up to the threshold of applicability of (8.3) or (6.3). We stress, however, that even if we have additional divergences that put a question mark near equations like (6.2), the mechanism is still the accumulation of dissipative contributions that ruin simple scaling.

Finally, we need to consider the implications of the findings in the context of this passive scalar model to the issue of the scaling theory of high Reynolds number turbulence. In a separate paper [25] it has been shown that in the case of Navier-Stokes turbulence the anomalous exponent turns out to be just too small to destroy the KO41 scaling in the structure functions in the limit of infinite Reynolds' number. However, due to its "dangerously irrelevant" nature, this field causes important corrections to scaling that do not go away even in atmospheric conditions. We shall argue that this picture

offers a self-contained description of all the known phenomenology in turbulence.

ACKNOWLEDGMENTS

We thank Bob Kraichnan for pointing out to us the possibilities inherent in the model studied in this paper, and for sharing with us his insights. It is a pleasure to acknowledge important discussions with Volodya Lebedev, whose valuable suggestions have contributed much to our understanding. This work has been supported in part by the U.S.-Israel Binational Science Foundation, the Israel Academy of the Sciences and the Humanities, and the Minerva Centre for Nonlinear Physics of Complex Systems.

APPENDIX A: TRANSFORMATION RULE FOR THE SHIFT OF THE ORIGIN OF THE QUASI-LAGRANGIAN COORDINATES

Define new variables $\tilde{\mathbf{v}}_{\mathbf{r}_0}(\mathbf{k}, t)$, $\tilde{\Theta}_{\mathbf{r}_0}(\mathbf{k}, t)$, and $\tilde{\phi}_{\mathbf{r}_0}$ according to

$$\tilde{\mathbf{v}}_{\mathbf{r}_0}(\mathbf{k}, t) = \mathbf{v}_{\mathbf{r}_0}(\mathbf{k}, t)e^{-i\mathbf{k}\cdot\mathbf{R}}, \quad (\text{A1})$$

$$\tilde{\Theta}_{\mathbf{r}_0}(\mathbf{k}, t) = \Theta_{\mathbf{r}_0}(\mathbf{k}, t)e^{-i\mathbf{k}\cdot\mathbf{R}}, \quad (\text{A2})$$

$$\tilde{\phi}_{\mathbf{r}_0}(\mathbf{k}, t) = \phi_{\mathbf{r}_0}(\mathbf{k}, t)e^{-i\mathbf{k}\cdot\mathbf{R}}. \quad (\text{A3})$$

The equation of motion in these variables reads

$$(\partial_t + \kappa k^2)\tilde{\Theta}_{\mathbf{r}_0} = i \int \frac{d\mathbf{k}_1}{(2\pi)^3} \frac{d\mathbf{k}_2}{(2\pi)^3} \tilde{\mathcal{V}}_{\mathbf{r}_0}(\mathbf{k}, \mathbf{k}_1, \mathbf{k}_2) \cdot \tilde{\mathbf{v}}_{\mathbf{r}_0}(\mathbf{k}_1, t)\tilde{\Theta}_{\mathbf{r}_0}(\mathbf{k}_2, t) + \tilde{\phi}_{\mathbf{r}_0}(\mathbf{k}, t), \quad (\text{A4})$$

where $\tilde{\mathcal{V}}_{\mathbf{r}_0}(\mathbf{k}, \mathbf{k}_1, \mathbf{k}_2)$ is a new vertex defined by

$$\tilde{\mathcal{V}}_{\mathbf{r}_0}(\mathbf{k}, \mathbf{k}_1, \mathbf{k}_2) = \mathcal{V}_{\mathbf{r}_0}(\mathbf{k}, \mathbf{k}_1, \mathbf{k}_2)e^{-i(\mathbf{k}+\mathbf{k}_1+\mathbf{k}_2)\cdot\mathbf{R}}. \quad (\text{A5})$$

Considering the definition (2.9), we see that

$$\tilde{\mathcal{V}}_{\mathbf{r}_0}(\mathbf{k}, \mathbf{k}_1, \mathbf{k}_2) = \mathcal{V}_{\mathbf{r}_0-\mathbf{R}}(\mathbf{k}, \mathbf{k}_1, \mathbf{k}_2). \quad (\text{A6})$$

Consequently the equation of motion of $\tilde{\Theta}_{\mathbf{r}_0}(\mathbf{k}, t)$ coincides with the equation of motion of $\Theta_{\mathbf{r}_0-\mathbf{R}}(\mathbf{k}, t)$. The correlation functions of the two fields must therefore be equal. In particular, if we define $\tilde{\mathcal{F}}_{\mathbf{r}_0}$ as the correlation function of the tilde variables, then

$$\tilde{\mathcal{F}}_{\mathbf{r}_0}(\mathbf{k}_1, \mathbf{k}_2, \omega_1) = \mathcal{F}_{\mathbf{r}_0-\mathbf{R}}(\mathbf{k}_1, \mathbf{k}_2, \omega_1). \quad (\text{A7})$$

From the definition of the tilde variables we have

$$\tilde{\mathcal{F}}_{\mathbf{r}_0}(\mathbf{k}_1, \mathbf{k}_2, \omega_1) = \mathcal{F}_{\mathbf{r}_0}(\mathbf{k}_1, \mathbf{k}_2, \omega_1)e^{i(\mathbf{k}_1+\mathbf{k}_2)\cdot\mathbf{R}}. \quad (\text{A8})$$

Combining these relations we get the transformation rule

$$\mathcal{F}_{\mathbf{r}_0-\mathbf{R}}(\mathbf{k}_1, \mathbf{k}_2, \omega_1) = \mathcal{F}_{\mathbf{r}_0}(\mathbf{k}_1, \mathbf{k}_2, \omega_1)e^{i(\mathbf{k}_1+\mathbf{k}_2)\cdot\mathbf{R}}. \quad (\text{A9})$$

This transformation rule reflects the space homogeneity of the equation of motion of $T(\mathbf{x}, t)$. The transformation rule for the Green's function of the scalar field is identical to (A9). Higher-order correlation functions will transform in an analogous fashion, simply by changing $(\mathbf{k}_1 + \mathbf{k}_2)$ in the exponent to the sum of wave vectors of $\tilde{\Theta}_{\mathbf{r}_0}$'s plus the sum of wave vectors of $\tilde{\Theta}_{\mathbf{r}_0}^*$'s. To get similar transformations for the velocity field one just needs to assume that its dynamical equation is also space homogeneous.

APPENDIX B: CALCULATION OF Σ

In order to show explicitly the dependence of the terms in the series for Σ , given by Eq. (2.23), on the ratio Γ/γ , we return to the calculation of the diagram $\Sigma^{(2)}$ given in Sec. III. In order to consider explicitly the frequency dependence we choose for definiteness a form for the scaling functions that captures the essence of the frequency behavior and allows the calculation to be performed sim-

ply. The scaling functions appearing in the definitions of the propagators (2.18) and (3.7) are taken to have the Lorentzian form

$$g\left(\frac{\omega}{\gamma_k}\right) = \frac{\gamma_k}{\omega + i\gamma_k}, \quad (\text{B1})$$

$$f\left(\frac{\omega}{\Gamma_k}\right) = \frac{\Gamma_k^2}{\omega^2 + \Gamma_k^2}. \quad (\text{B2})$$

This is known as the one-pole approximation. The details of this choice are not important for the result, but merely serve to simplify the computation.

Let us begin by calculating $\Sigma^{(2)}$. Integrating out the second \mathbf{k} -vector dependence of the Green's function one obtains

$$\begin{aligned} \Sigma^{(2)}(\mathbf{k}_1, \mathbf{k}_2, \omega) = & \int \frac{d\mathbf{p}}{(2\pi)^3} \frac{d\mathbf{q}}{(2\pi)^3} \frac{d\omega_1}{2\pi} \mathcal{V}(\mathbf{k}_1, \mathbf{q}, \mathbf{p}) \\ & \cdot \mathcal{H}(\mathbf{q}, \omega - \omega_1) \cdot \mathcal{V}(\mathbf{p}, \mathbf{q}, \mathbf{k}_2) \\ & \times G(\mathbf{p}, \omega - \omega_1), \end{aligned} \quad (\text{B3})$$

where $G(\mathbf{k}, \omega)$ is defined by (3.5). Now inserting the scaling forms (B1) and (B2), let us consider only the integration over the frequency

$$S(\omega) = \int \frac{d\omega_1}{2\pi} \frac{\Gamma_q}{\omega_1^2 + \Gamma_q^2} \frac{1}{\omega - \omega_1 + i\gamma_p}. \quad (\text{B4})$$

Closing the contour of integration in the lower half plane gives $\omega_1 = -i\Gamma_q$; then using the limit $\Gamma \gg \gamma \sim \omega$, we recover the frequency-independent result of the calculation of Sec. III, but now with the explicit coefficient $S(\omega) \sim \Gamma_p$. Therefore

$$\begin{aligned} \Sigma^{(2)}(\mathbf{k}_1, \mathbf{k}_2) = & -i \int \frac{d\mathbf{p}}{(2\pi)^3} \frac{d\mathbf{q}}{(2\pi)^3} \mathcal{V}(\mathbf{k}_1, \mathbf{q}, \mathbf{p}) \cdot \mathbf{P}_q \\ & \cdot \mathcal{V}(\mathbf{p}, \mathbf{q}, \mathbf{k}_2) \frac{H(q)}{\Gamma_q}. \end{aligned} \quad (\text{B5})$$

To proceed, let us estimate the k dependence by assuming that the major contribution results from $k_1 \sim k_2 \sim k$, and using locality. Therefore we find that

$$\gamma_k \equiv \text{Im}\Sigma^{(2)} \sim \frac{k^5 H(k)}{\Gamma_k}. \quad (\text{B6})$$

Now consider the second-order diagram as displayed in Fig. 13. After integrating out one of the k vectors of each Green's function and performing the δ functions

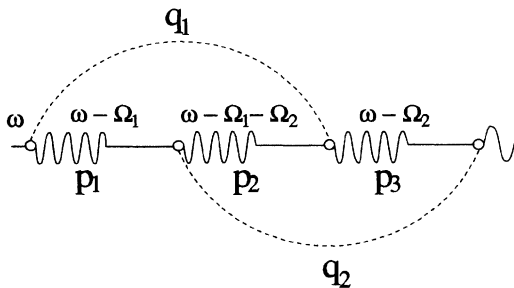


FIG. 13. $\Sigma^{(3)}$.

over frequencies, we are left with two independent frequency integrations and five k integrations (dependent due to the vertices):

$$\begin{aligned} \Sigma^{(3)}(\mathbf{k}_1, \mathbf{k}_2, \omega) = & \int \frac{d\mathbf{q}_1}{(2\pi)^3} \frac{d\mathbf{q}_2}{(2\pi)^3} \prod_3^{m=1} \frac{d\mathbf{p}_m}{(2\pi)^3} \mathcal{V}(\mathbf{k}_1, \mathbf{q}_1, \mathbf{p}_1) \\ & \cdot \mathcal{H}(\mathbf{q}_1, \Omega_1) \cdot \mathcal{V}(\mathbf{p}_1, \mathbf{q}_2, \mathbf{p}_2) \mathcal{H}(\mathbf{q}_2, \Omega_2) \\ & \cdot \mathcal{V}(\mathbf{p}_3, \mathbf{q}_2, \mathbf{k}_2) G(\mathbf{p}_1, \omega - \Omega_1) \\ & \times G(\mathbf{p}_2, \omega - \Omega_1 - \Omega_2) G(\mathbf{p}_3, \omega - \Omega_2). \end{aligned} \quad (\text{B7})$$

Isolating the frequency integration as above results in

$$\begin{aligned} S(\omega) = & \int \frac{d\Omega_1}{2\pi} \frac{d\Omega_2}{2\pi} \frac{1}{(\omega - \Omega_1 + i\gamma_1)} \\ & \times \frac{1}{(\omega - \Omega_1 - \Omega_2 + i\gamma_2)} \\ & \times \frac{1}{(\omega - \Omega_2 + i\gamma_3)} \frac{\Gamma_1}{\Omega_1^2 + \Gamma_1^2} \frac{\Gamma_2}{\Omega_2^2 + \Gamma_2^2}, \end{aligned} \quad (\text{B8})$$

where $\gamma_i \equiv \gamma_{p_i}$, $\Gamma_i \equiv \Gamma_{q_i}$. Integrating first over Ω_1 , there is one pole in the lower half plane, $\Omega_1 = -i\Gamma_1$, and similarly $\Omega_2 = -i\Gamma_2$. Therefore the result, again neglecting γ with respect to Γ , is

$$S(\omega) \sim \frac{1}{\Gamma_k^3}. \quad (\text{B9})$$

Again estimating the k dependence using locality gives for the total

$$\Sigma^{(3)} \sim \frac{[k^5 H(k)]^2}{\Gamma^3}, \quad (\text{B10})$$

which, making use of Eq. (B6), shows that

$$\Sigma^{(3)} \sim \Sigma^{(2)} \frac{\gamma_k}{\Gamma_k}. \quad (\text{B11})$$

We stress again that this coefficient is a result of the structure of the diagrams and the limit $\Gamma \gg \gamma$, and is independent of the particular choice for f and g .

APPENDIX C: SYMMETRY OF THE GREEN'S FUNCTION

We can rewrite Eq. (2.21) in the form

$$\mathcal{G}_0^{-1} \mathcal{G}_{12} = (2\pi)^3 \delta(\mathbf{k}_1 + \mathbf{k}_2) + \Sigma_{13} \mathcal{G}_{32}, \quad (\text{C1})$$

$$\mathcal{G}_0^{-1} \mathcal{G}_{21} = (2\pi)^3 \delta(\mathbf{k}_1 + \mathbf{k}_2) + \Sigma_{23} \mathcal{G}_{31}, \quad (\text{C2})$$

where we use the shorthand notation introduced in Sec. IIIB. In Eq. (C1) we can use the fact that the Dyson equation can be resummed from either the left or the right, and an equivalent form to (C1) is

$$\mathcal{G}_0^{-1} \mathcal{G}_{12} = (2\pi)^3 \delta(\mathbf{k}_1 + \mathbf{k}_2) + \mathcal{G}_{13} \Sigma_{32}. \quad (\text{C3})$$

Since Σ is symmetric [cf. Eq. (3.4)] we subtract (C2)

from (C3) to obtain

$$\int \frac{d\mathbf{k}_3}{(2\pi)^3} \Delta \mathcal{G}_{13} [(2\pi)^3 \mathcal{G}_0^{-1} \delta(\mathbf{k}_1 + \mathbf{k}_2) - \Sigma_{23}] = 0, \quad (\text{C4})$$

where $\Delta \mathcal{G}_{13} = \mathcal{G}_{13} - \mathcal{G}_{31}$. Noticing that \mathcal{G}_0^{-1} is a function of ω while it has been shown that Σ_{23} is not, we conclude that $\Delta \mathcal{G}_{13}$ must vanish.

APPENDIX D: THE ASYMPTOTIC PROPERTIES OF THE TWO-POINT PROPAGATORS AND THE FREQUENCY CONVERGENCE OF THE DIAGRAMS

To find the asymptotic properties for large frequencies of the Green's function $\mathcal{G}(\mathbf{k}_1, \mathbf{k}_2, \omega)$ assume first that its real part is much larger than its imaginary part when $\omega \rightarrow \infty$. From Eq. (3.4) we then see that

$$\begin{aligned} \mathcal{G}'(\mathbf{k}_1, \mathbf{k}_2, \omega) &= \mathcal{G}'_0(\mathbf{k}_1, \mathbf{k}_2, \omega) \\ &= (2\pi)^3 \delta(\mathbf{k}_1 + \mathbf{k}_2) / \omega \sim 1/\omega. \end{aligned} \quad (\text{D1})$$

It is clear from Eq. (3.6) that this form will also hold for the integrated Green's function (3.5). We proceed now to analyze the imaginary part of (3.5), $G''(\mathbf{k}, \omega)$. The imaginary part of Eq. (3.6) gives

$$\begin{aligned} \omega G''(\mathbf{k}_1, \mathbf{k}_2, \omega) &= k^2 \int \frac{d\mathbf{q}}{(2\pi)^3} \sin^2 \theta_{kq} \mathcal{H}(q) \\ &\quad \times [G(\mathbf{q} - \mathbf{k}, \omega) - G(\mathbf{k}, \omega)]. \end{aligned} \quad (\text{D2})$$

We have previously introduced for $G(k, \omega)$ the scaling form (3.7). In the asymptotic regime of large ω ($\omega \gg k^z$), we take the form

$$G''(k, \omega) \propto \frac{1}{k^z} \left(\frac{\omega}{k^z} \right)^{-\alpha}, \quad (\text{D3})$$

where the exponent α is to be determined. There are two relevant regimes in the evaluation of the integral (D2): the region $q \sim k$, and the region $q^z \sim \omega$, i.e., $q \gg k$. In the first case, we invoke the asymptotic form $G(k, \omega) \sim 1/\omega$, and realize that this contribution will be small due to the cancellation of the leading order terms. In the regime $q \gg k$, $G(\mathbf{k}, \omega)$ is already in the asymptotic regime and is negligible in comparison with $G(\mathbf{k} - \mathbf{q}, \omega) \sim G(\mathbf{q}, \omega)$ which as $q^z \sim \omega$ is *not* asymptotic. Therefore the integrand reduces to a function of q only, and the integral is proportional to k^2 due to the prefactor. Now we may determine the exponent α by balancing powers of k . The result is

$$\alpha = \frac{2+z}{z}. \quad (\text{D4})$$

Therefore in the limit $\omega \rightarrow \infty$, the imaginary part of the Green's function indeed falls off faster than the real part, according to

$$G''(k, \omega) \propto \frac{1}{\omega^{(2+z)/z}}. \quad (\text{D5})$$

Turning now to the correlation function, we use Wyld's

equation (2.22). Replacing again the Green's function by its real part and using the independence of Φ on frequency, we conclude that for large frequencies

$$\mathcal{F}(\mathbf{k}_1, \mathbf{k}_2, \omega) \sim 1/\omega^2. \quad (\text{D6})$$

Next we prove that the integrals of the propagators over frequency exist with the scaling forms assumed for them. In other words, we need to prove that the simultaneous propagators exist in the sense that they are independent of the viscous cutoff. For the Green's function this is immediate because of the frequency sum rule (3.2). For small frequencies it follows from the fact that $\mathcal{F}(\mathbf{k}_1, \mathbf{k}_2, \omega)$ is finite. This follows directly from Eq. (C1), using that \mathcal{G} is finite at $\omega = 0$ [cf. (3.5)], and that Φ is frequency independent.

Having established these properties, we can show now that all the integrals with respect to frequency in our diagrammatic expansion converge. Let us start with Σ . The way to see the convergence is to note that the number of independent integrations with respect to frequency is always the same as the number of correlators. Therefore, we can choose as the independent frequencies of integration the frequencies of the correlators, making the frequencies of the Green's functions linear combinations of the above. Since the Green's functions are bounded for any frequency, the convergence of any diagram is guaranteed if the integral over the correlator itself is bounded. The latter is guaranteed whenever the correlator is $\mathcal{F}(\mathbf{k}_1, \mathbf{k}_2, \omega)$ by the properties given above. However when the correlator is \mathcal{H} , we need to discuss the issue further, since we took \mathcal{H} as frequency independent, and the integral of \mathcal{H} is therefore unbounded. On the other hand, as argued above, the \mathcal{H} correlators appear in all the diagrams as vertical dashed lines. This means that each loop contains exactly two Green's functions, except in the first diagram, where there is only one (see Fig. 3). In this first diagram, the frequency integral converges due to the sum rule (3.2). In all the other diagrams the two Green's functions in every loop ensure convergence due to their asymptotic properties (D1) and (D5), and the finiteness of $\mathcal{G}(\mathbf{k}_1, \mathbf{k}_2, \omega = 0)$.

In the series for Φ we have one additional correlator $\mathcal{F}(\mathbf{k}_1, \mathbf{k}_2, \omega)$ in every independent integration. Given the asymptotic properties of $\mathcal{F}(\mathbf{k}_1, \mathbf{k}_2, \omega)$ it is easy to see that the above argument is not destroyed.

APPENDIX E: THE IMAGINARY PART OF THE GREEN'S FUNCTION

We will use the following fact concerning the imaginary part of a product of functions $\alpha\beta\gamma\delta \dots$:

$$\begin{aligned} (\alpha\beta\gamma\delta \dots)'' &= \frac{\alpha\beta\gamma\delta \dots - \alpha^*\beta^*\gamma^*\delta^* \dots}{2i} \\ &= -(\alpha''\beta^*\gamma^*\delta^* \dots + \alpha\beta''\gamma^*\delta^* \dots \\ &\quad + \alpha\beta\gamma''\delta^* \dots + \dots), \end{aligned} \quad (\text{E1})$$

which can be verified directly by replacing each α with $\frac{\alpha - \alpha^*}{2i}$. The Dyson equation (2.21) may be expanded dia-

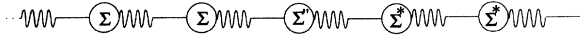


FIG. 14. Expansion of the imaginary part of the Green's function.

grammatically as in Fig. 3(a). Performing the expansion (E1), one replaces every term in the above with combinations of terms of the form shown in Fig. 14.

Resumming the series one finds that

$$\mathcal{G}_{12}'' = \mathcal{G}_0'' + \mathcal{G}_{13}\Sigma_{34}''\mathcal{G}_{24}^*. \quad (\text{E2})$$

Neglecting the small term κk^2 we end up with (3.13).

APPENDIX F: THE LOCALITY OF $\mathcal{D}_2(\mathbf{R})$

Examine the integral (5.12) in the case $n = 2$,

$$\begin{aligned} \mathcal{D}_2(\mathbf{r}) = & \frac{(2\pi)^3}{2} \int \frac{d\mathbf{k}}{(2\pi)^3} \frac{d\mathbf{q}_1}{(2\pi)^3} \frac{d\mathbf{q}_2}{(2\pi)^3} |1 - \exp(i\mathbf{q}_1 \cdot \mathbf{r})|^2 \\ & \times [\mathbf{q}_2 \cdot \mathcal{H}(\mathbf{k}) \cdot \mathbf{q}_1] [F(q_1) - F(q_2)] \\ & \times \delta(\mathbf{k} + \mathbf{q}_1 + \mathbf{q}_2). \end{aligned} \quad (\text{F1})$$

The ir convergence is analyzed by examining the range of

integration in which either one of the three \mathbf{k} vectors is much smaller than the other two, or all three are small, and of the same order. If k is much smaller, then q_1 and q_2 are approximately equal, making the difference $F(q_1) - F(q_2)$ small. Expanding this difference in k , the linear order vanishes after integration, and the second order contributes an integral $\int k^2 H(k) dk$ which is convergent in the ir in our case. In the case q_2 small, the factor $\mathbf{q}_2 \cdot \mathcal{H}(\mathbf{k}) \cdot \mathbf{q}_1$, which can be written equivalently as $\mathbf{q}_2 \cdot \mathcal{H}(\mathbf{k}) \cdot \mathbf{q}_2$, contributes the most dangerous contribution $q_2^2 F(q_2) dq_2$, which is again convergent in the ir. The case q_1 small is less dangerous since then the term $|1 - \exp(i\mathbf{q}_1 \cdot \mathbf{r})|^2$ contributes an additional factor of q_1^2 . Lastly, the case k, q_1, q_2 small and of the same order is estimated by power counting to be convergent since $\int q^9 H(q) F(q) dq$ is ir convergent.

In the uv regime we have either two large \mathbf{k} vectors and one small, or three large \mathbf{k} vectors. Take q_1 and q_2 large, and of order $q \gg k$. The factor $\mathbf{q}_2 \cdot \mathcal{H}(\mathbf{k}) \cdot \mathbf{q}_2$ contributes q^2 . The factor $[F(q_1) - F(q_2)]$ contributes, after expansion, $k^2 F(q)/q^2$. One integration over q is taken care of by the δ function, and we end up with $k^2 \int F(q) dq$ which is convergent in the uv. Now with k and either q_1 or q_2 large and of the same order, the dangerous integral is $\int H(k) F(k) dk$, which converges in the uv.

-
- [1] A. N. Kolmogorov, Dokl. Akad. Nauk. SSSR **31**, 538 (1941).
 [2] A. M. Obukhov, Dokl. Akad. Nauk. SSSR **32**, 229 (1941).
 [3] H. Tennekes and J. C. Wyngaard, J. Fluid Mech. **55**, 93 (1972).
 [4] C. W. Van Atta and R. A. Antonia, Phys. Fluids **23**, 252 (1980).
 [5] F. Anselmet, Y. Gagne, E. J. Hopfinger, and A. R. Antonia, J. Fluid Mech. **140**, 63 (1984).
 [6] A. M. Obukhov, Izv. Akad. Nauk SSSR Ser., Geogr. Geofiz. **13**, 58 (1949).
 [7] S. Corrsin, J. Appl. Phys. **22**, 469.
 [8] K. R. Sreenivasan, Annu. Rev. Fluid Mech. **23**, 539 (1991).
 [9] R. Benzi, S. Ciliberto, R. Trippicione, C. Baudet, F. Masaioli, and S. Succi, Phys. Rev. E **48**, R29 (1993).
 [10] A. N. Kolmogorov, J. Fluid Mech. **13**, 82 (1962).
 [11] E. A. Novikov and R. W. Stewart, Izv. Geofiz. **3**, 408 (1964).
 [12] A. S. Gurvich and S. L. Zubkovski, Izv. Akad. Nauk. SSSR Ser., Geofiz. **2**, 1856 (1963).
 [13] B. B. Mandelbrot, J. Fluid Mech. **62**, 331 (1974).
 [14] U. Frisch, P. Sulem, and M. Nelkin, J. Fluid Mech. **87** 719 (1978).
 [15] U. Frisch and G. Parisi, in *Turbulence and Predictability in Geophysical Fluid Dynamics and Climate Dynamics*, edited by M. Ghil, R. Benzi, and G. Parisi (North-Holland, New York, 1985), p. 84.
 [16] R. H. Kraichnan, Phys. Fluids **8**, 575 (1965).
 [17] V. I. Belinicher and V. S. L'vov, Zh. Eksp. Teor. Fiz. **93**, 533 (1987) [Sov. Phys. JETP **66**, 303 (1987)].
 [18] V. S. L'vov, Phys. Rep. **207**, 1 (1991).
 [19] V. V. Lebedev and V. S. L'vov, Pis'ma Zh. Eksp. Teor. Fiz. **59**, 546 (1994) [JETP Lett. **59**, 577 (1994)].
 [20] P. Constantin and I. Procaccia, Phys. Rev. E **47**, 3307 (1993).
 [21] P. Constantin and I. Procaccia, Nonlinearity **7**, 1045 (1994).
 [22] R. H. Kraichnan, Phys. Rev. Lett. **72**, 1016 (1994).
 [23] R. H. Kraichnan, Phys. Fluids **11**, 945 (1968).
 [24] H. W. Wyld, Ann. Phys. (N.Y.) **14**, 143 (1961).
 [25] V. S. L'vov and I. Procaccia (unpublished).
 [26] See, for example, B. L. Altshuler and A. G. Aronov, in *Electron-Electron Interactions in Disordered Systems*, edited by A. L. Efros and M. Pollak (Elsevier, New York, 1985), p. 1.
 [27] R. H. Kraichnan, Phys. Fluids **9**, 1728 (1966).
 [28] V. E. Zakharov, Zh. Eksp. Teor. Fiz. **51**, 688 (1966) [Sov. Phys. JETP **24**, 455 (1967)].
 [29] A. Kats and V. Kontorovich, Zh. Eksp. Teor. Fiz. **64**, 153 (1973) [Sov. Phys. JETP **37**, 80 (1973)].